International Geology Review
Publication details, including instructions for authors and subscription information:
http://www.tandfonline.com/loi/tigr20

Petrology, geochemistry, and tectonic significance of Mesozoic shoshonitic volcanic rocks, Luzong volcanic basin, eastern China

Jianghong Deng [a b], Xiaoyong Yang [a b], Weidong Sun [c a], Yu Huang [d], Yueyu Chi [e], Liangfan Yu [e] & Qianming Zhang [e]

[a] CAS Key Laboratory of Crust-Mantle Materials and Environments, University of Science and Technology of China, Hefei, 230026, PR China

[b] State Key Laboratory of Ore Deposit Geochemistry, Institute of Geochemistry, Chinese Academy of Sciences, Guiyang, 550002, PR China

[c] CAS Key Laboratory of Isotope Geochronology and Geochemistry, Guangzhou Institute of Geochemistry, Chinese Academy of Sciences, Guangzhou, 510640, PR China

[d] Department of Geology, University of Maryland, College Park, Maryland, 20742, USA

[e] No. 327 Geological Team, Anhui Bureau of Land and Mineral Resources, Hefei, 230001, PR China

Published online: 10 Jun 2011.

To cite this article: Jianghong Deng , Xiaoyong Yang , Weidong Sun , Yu Huang , Yueyu Chi , Liangfan Yu & Qianming Zhang (2012) Petrology, geochemistry, and tectonic significance of Mesozoic shoshonitic volcanic rocks, Luzong volcanic basin, eastern China, International Geology Review, 54:6, 714-736, DOI: 10.1080/00206814.2011.580628

To link to this article: http://dx.doi.org/10.1080/00206814.2011.580628

International Geology Review
Vol. 54, No. 6, 20 April 2012, 714–736

Taylor & Francis
Taylor & Francis Group

Petrology, geochemistry, and tectonic significance of Mesozoic shoshonitic volcanic rocks, Luzong volcanic basin, eastern China

Jianghong Deng[a,b], Xiaoyong Yang[a,b*], Weidong Sun[c,a], Yu Huang[d], Yueyu Chi[e], Liangfan Yu[e] and Qianming Zhang[e]

[a]*CAS Key Laboratory of Crust-Mantle Materials and Environments, University of Science and Technology of China, Hefei 230026, PR China;* [b]*State Key Laboratory of Ore Deposit Geochemistry, Institute of Geochemistry, Chinese Academy of Sciences, Guiyang 550002, PR China;* [c]*CAS Key Laboratory of Isotope Geochronology and Geochemistry, Guangzhou Institute of Geochemistry, Chinese Academy of Sciences, Guangzhou 510640, PR China;* [d]*Department of Geology, University of Maryland, College Park, Maryland 20742, USA;* [e]*No. 327 Geological Team, Anhui Bureau of Land and Mineral Resources, Hefei 230001, PR China*

(*Accepted 17 March 2011*)

We studied the geochemical characteristics of three types of Mesozoic igneous rocks from the Luzong volcanic basin: basaltic trachyandesite at Shuangmiao, pyroxene monzonite at Bajiatan, and quartz-syenite (A-type granite) at Huangmeijian. Based on analyses of whole-rock major elements, all investigated rocks are enriched in K, Na, Ti, Al, but depleted in Ca, representing a shoshonitic series. Trace element analyses show that these rocks are characterized by enrichments of large-ion lithophile elements and high field strength elements. Positive Nb and Ta anomalies in the chondrite-normalized spider diagram indicate that the shoshonitic volcanic rocks share similar features with Nb-enriched basalts, which are different from normal island-arc volcanical rocks (they are typically strongly depleted in Nb and Ta). Bulk-rock chemical compositions and Sr–Nd isotopes indicate that the three types of igneous rocks are geochemically comagmatic, suggesting that the melts were derived from an enriched mantle reservoir. We postulate an extensional tectonic setting for the formation of Luzong volcanic basin, possibly related to subduction of a palaeo-Pacific plate beneath the east Chinese continent during the Yanshanian period (Cretaceous). Therefore, the petrogenetic features of those volcanic rocks as well as A-type granites in the Luzong basin indicate that the regional large-scale Fe–Cu–Au mineralization was associated with oceanic slab melting, but not delamination or recycling of the ancient lower continental crust, as previously proposed.

Keywords: tectonic environment; shoshonite; Nb-enriched basalt; Luzong volcanic basin; Pacific plate subduction

Introduction

From north to south, eastern China can be divided into several tectonic units, that is, the North China craton, the Dabie-Sulu orogenic belt, the Yangtze Block and the Cathaysian block; each of these units is characterized by unique geological-tectonic evolutionary patterns from basements to caprocks. The Middle-Lower Yangtze River area is located near the junction of the Yangtze Block and North China craton. It is an important magmatic-metallogenic belt (Chang *et al*. 1991; Zhai *et al*. 1992, 1996; Tang *et al*. 1998; Pan and Dong 1999; Mao *et al*. 2006; Yang *et al*. 2011), where the development of late Mesozoic magmatic rocks from ultramafic to felsic and alkaline series was extensive. Studying the geochemical characteristics of igneous rocks along the metallogenic belt can set significant constraints to our understanding of the late Mesozoic crust–mantle evolution in eastern China.

Many researchers have extensively studied the formation ages, geochemical characteristics, magmatic processing, and tectonic environments of the late Mesozoic igneous rocks in the Middle-Lower Yangtze metallogenic belt (e.g. Chang *et al*. 1991; Ren *et al*. 1991; Zhai *et al*. 1992; Wang *et al*. 1996; Pan and Dong 1999; Xing and Xu 1999; Liu *et al*. 2002; Wu *et al*. 2003; Zhang *et al*. 2003; Mao *et al*. 2006; Wang *et al*. 2006; Zhou *et al*. 2007, 2008 Yang *et al*. 2011). However, controversies related to the formation of these magmatic rocks remain poorly clarified, especially regarding the tectonic settings. Some scholars have proposed a Pacific plate subduction-related genesis (Deng *et al*. 1992; Wang *et al*. 2004; Sun *et al*. 2007; Liu *et al*. 2010); others have suggested an intraplate extensional rift environment (Xing and Xu 1999); yet other researchers have favoured a transitional tectonic setting between continental margin environment and intracontinental block environment (Chen *et al*. 2001; Chen *et al*. 2005).

Magmatic rocks in the Middle-Lower Yangtze metallogenic belt are mainly classified as three series: (1) a high-K calc-alkaline series, mainly developed in uplifted areas such as the Tongling and Anqing regions (Chang *et al*. 1991); (2) a shoshonite series, normally formed in faulted volcanic basins represented by the Luzong and

*Corresponding author. Email: xyyang555@163.com

ISSN 0020-6814 print/ISSN 1938-2839 online

http://dx.doi.org/10.1080/00206814.2011.580628
http://www.tandfonline.com

Nanjing-Wuhu areas (Ren *et al*. 1991; Wang *et al*. 1996); (3) A-type granitoids (alkaline intrusive rocks and granite), distributed along the Yangtze River fault, both in the uplift zones and in the fault zones (Xing and Xu 1999). Zhang *et al*. (1998) and Xing and Xu (1999) conducted a preliminary study on A-type granitoids, and they confirmed that there are two A-type granite belts extending from north to south in Anhui Province. Some scholars believe that the water-bearing A-type granite belt could serve as the host of porphyry copper deposits under certain conditions in the Ailaoshan-Jinshajiang fault zone, SW China (Bi *et al*. 2000; Bi *et al*. 2005).

Yu and Bai (1981) first proposed the presence of a Mesozoic shoshonitic volcanic province in the Luzong region, with 70% of the surficial exposures as intermediate rocks and less than 30% as mafic rocks. Large-scale Fe–Cu–Au mineralization in the Luzong Basin is associated with these igneous series (Ren *et al*. 1991; Yang 1996; Yang *et al*. 2002, 2006, 2007, 2011; Yang and Lee 2005). Some geologists have proposed that both igneous rocks and poly-metal mineralization in the Luzong volcanic basin are resulted from the delamination and recycling of the ancient lower continental crust (Wang *et al*. 2001, 2004, 2006). Our research mainly focused on these shoshonitic rocks and A-type granitic plutons in the Luzong Basin in central Anhui Province along the north margin of the Yangtze River (Figure 1). We attempt to investigate the sources of shoshonitic magma and determine the tectonic environment for the formation of the Luzong volcanic basin, employing geochemical constraints. Our results indicate a Pacific plate subduction-related tectonic setting during the Yanshanian period (Cretaceous) for the generation of the shoshonitic series in this volcanic basin.

Regional geological background

Regional geology

The Luzong volcanic basin, covering an area c.a. 1032 km^2, is located in the Middle-Lower Yangtze region, with its SE margin as Yangtze Craton and NW margin as North China Craton. This basin is enclosed by three boundary faults: the NNE Luohe – Peigang-Liantan fault, the NEE Yangtze River fault, and the Xiangan-Datong fault (Figure 2). Intensive volcanic activities occurred in the late Mesozoic and formed a set of shoshonitic volcanic rocks and A-type granitoids at Luzong basin region, locally referred as the Longmenyuan Group, the Zhuanqiao Group, the Shuangmiao Group, and the Fushan Group (Figure 2). Exposed volcanic rocks in the basin cover an area about 800 km^2, consisted of 21% basaltic rocks, 26% basaltic-trachyandesitic volcanic rocks, 44% trachyandesite, and 9% trachyte (Yu and Bai 1981; Deng *et al*. 1992).

A-type granite plutons in Luzong basin are mainly distributed along the Yangtze River fault with NE direction, including the Chengshan–Zongyang intrusion and the Huangmeijian intrusion. Some smaller A-type granitoids, whose surficial exposure area is about 277 km^2, are also spread within the basin, such as the Fanshan and Bajiatan stocks. Most of these A-type granitoids are quartz-syenite (porphyry) and syenite (porphyry), which cover more than 265 km^2 together. Minor A-type granitoids are pyroxene monzonite (mainly found in Bajiatan stock

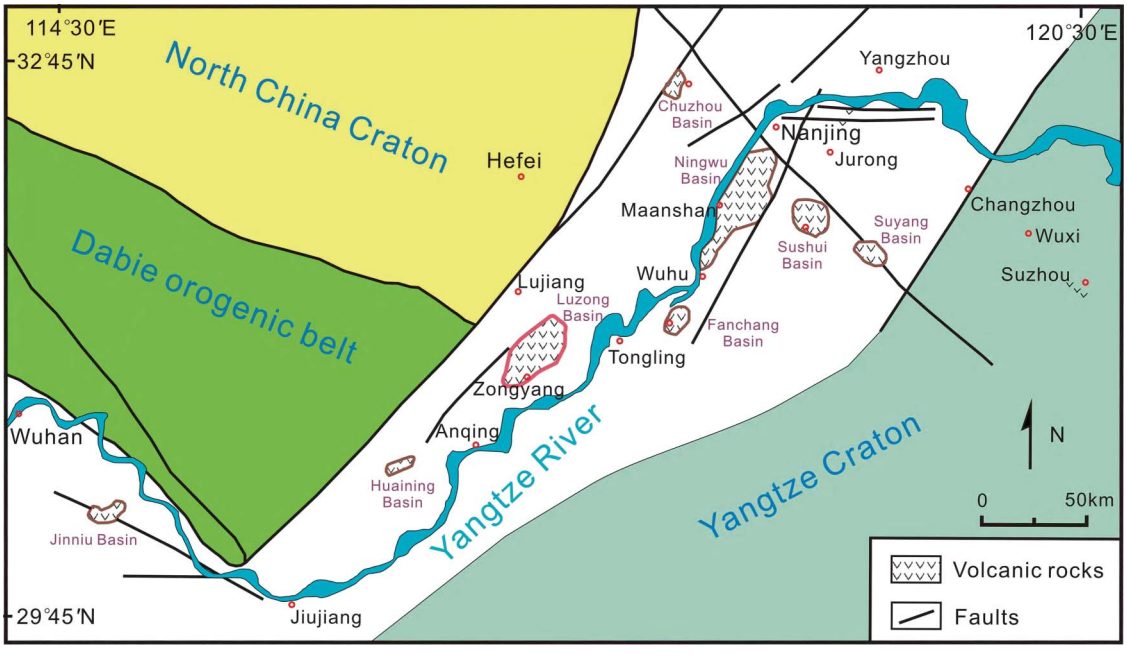

Figure 1. Sketch map of volcanic basin areas along Yangtze River (modified after Zhou *et al*. (2008) and Zhai *et al*. (1992)).

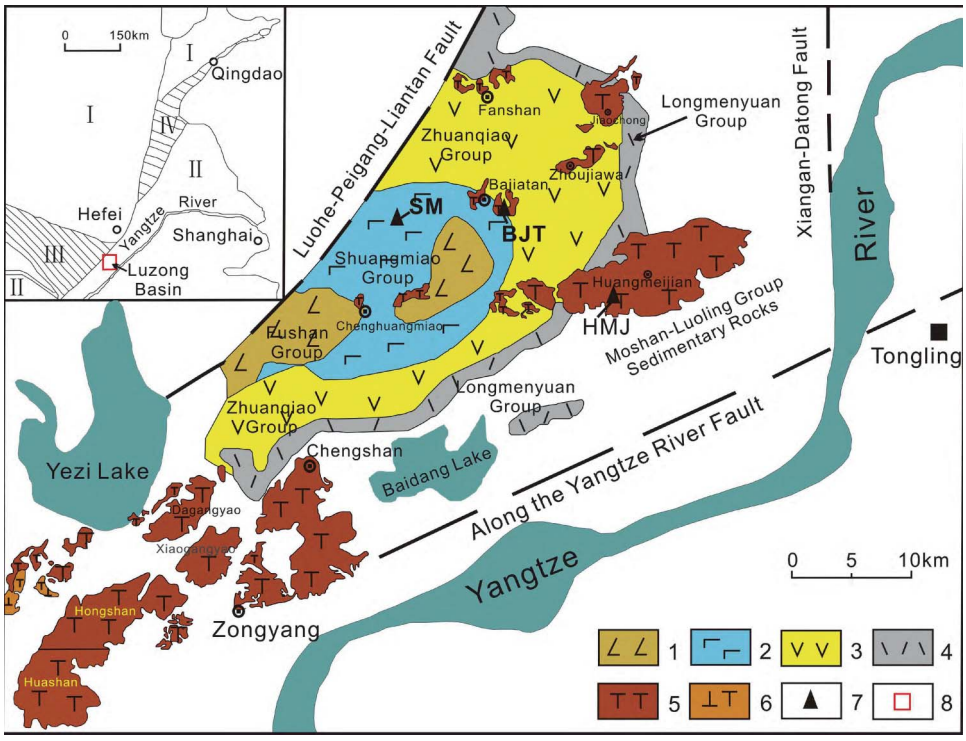

Figure 2. The distribution of Luzong basin Mesozoic volcanic-intrusive rocks, Anhui, China (modified after Cao *et al*. 2008; Liu *et al*. 2002). Note: SM, Shuangmiao Group; BJT, Bajiatan intrusion; HMJ, Huangmeijian A-type granite. 1. Fushan Group volcanic rocks; 2. Shuangmiao Group volcanic rocks; 3. Zhuanqiao Group volcanic rocks; 4. Longmenyuan Group volcanic rocks; 5. syenitic–monzonitic intrusive rocks; 6. syenitic diorites; 7. sampling sites; 8. research area. I, North China plate; II, Yangtze plate; III, Dabie orogenic belt; IV, Sulu orogenic belt.

with an exposure area about 4 km^2), quartz-monzonite (porphyry), and alkali-feldspar granite (<1 km^2 exposure area) (Zhang *et al*. 1988). These plutonic rocks mainly consist of complexes, with some homology xenoliths exhibiting intrusion–contact relationships with the overlying Mesozoic volcanic rocks (Zhang *et al*. 1988; Ren *et al*. 1991; Yang *et al*. 1993; Zheng *et al*. 1997).

Twenty-five volcanic rock samples were collected from the Shuangmiao Group, Huangmeijian, and Bajiatan stocks to investigate their geochemical characteristics (Figure 2).

Description of igneous rocks

Shuangmiao group rocks

Volcanic rocks in the Luzong volcanic basin were accumulated by four eruption stages in the Early Cretaceous, that is, the Longmenyuan, Zhuanqiao, Shuangmiao, and Fushan cycles, corresponding to the generations of Longmenyuan Group, Zhuanqiao Group, Shuangmiao Group, and Fushan Group volcanic rocks, respectively (Chang *et al*. 1991; Ren *et al*. 1991; Tang *et al*. 1998) (Figure 3). Zircon LA-(inductively coupled plasma-mass spectrometry) ICP-MS dating of volcanic rocks demonstrated that the formation ages of the referred four groups in this basin are 135 Ma, 134 Ma, 130 Ma, and 126 Ma, respectively (Zhou *et al*. 2008).

Volcanic rocks of Shuangmiao Group are mainly trachybasalt, trachyandesite, and trachyte volcanic rocks, and show an unconformity contact relationship with the underlying Zhuanqiao Group. On the basis of lithology, Shuangmiao Group can be divided into three main sections:

Top: mainly black-grey trachybasalts, basaltic trachyandesites, and mixed tuffaceous siltstones;

Middle: mainly grey trachybasalts, purple-red tuffaceous siltstones, breccia-containing trachybasalts, trachybasaltic breccia lava, trachyte and olive trachybasalt in parts;

Bottom: mainly purple-red siltstones (including calcium-TB), tuffaceous siltstones, tuff breccias, and agglomerates.

Bajiatan intrusion

Bajiatan intrusion is located at Zhuanqiao town in the centre of Luzong volcanic basin with an oval-shaped exposure area of about 4 km^2 (Figure 2). This plutonic body intruded into existing Jurassic volcanic rocks at about 133.5 ± 0.6 Ma in Early Cretaceous time as given by SHRIMP zircon U-Pb dating (Zhou *et al*. 2007). According to lithology and contact relationship, Bajiatan rocks are divided into two phases, that is, the centre and the edge, corresponding to different rock types, that is, pyroxene monzonite and quartz

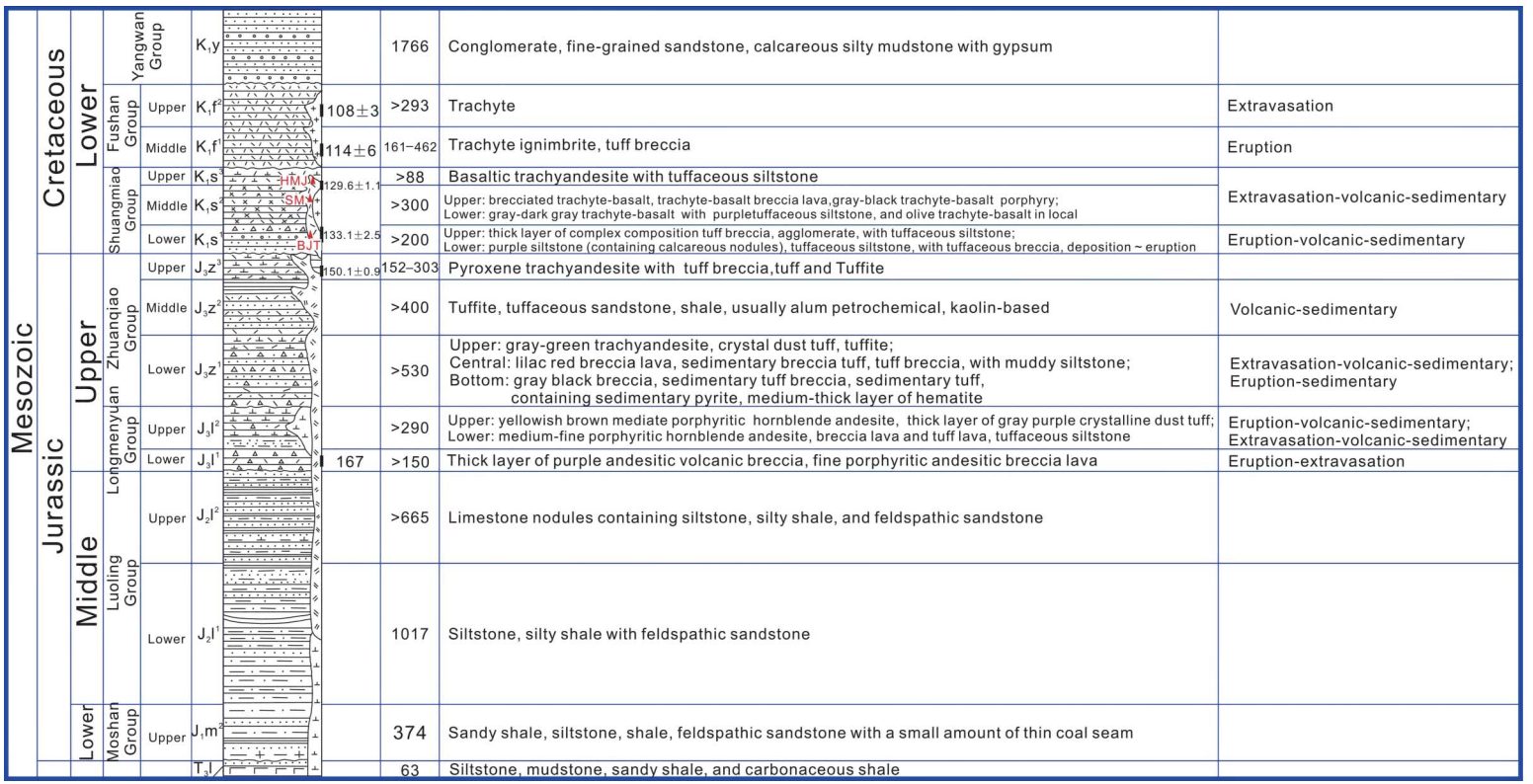

Mesozoic	Cretaceous	Lower	Yangwan Group		K_1y			1766	Conglomerate, fine-grained sandstone, calcareous silty mudstone with gypsum	
			Fushan Group	Upper	K_1f^2		108±3	>293	Trachyte	Extravasation
				Middle	K_1f^1		114±6	161–462	Trachyte ignimbrite, tuff breccia	Eruption
			Shuangmiao Group	Upper	K_1s^3	HMJ	129.6±1.1	>88	Basaltic trachyandesite with tuffaceous siltstone	Extravasation-volcanic-sedimentary
				Middle	K_1s^2	SM		>300	Upper: brecciated trachyte-basalt, trachyte-basalt breccia lava,gray-black trachyte-basalt porphyry; Lower: gray-dark gray trachyte-basalt with purpletuffaceous siltstone, and olive trachyte-basalt in local	
				Lower	K_1s^1	BJT	133.1±2.5	>200	Upper: thick layer of complex composition tuff breccia, agglomerate, with tuffaceous siltstone; Lower: purple siltstone (containing calcareous nodules), tuffaceous siltstone, with tuffaceous breccia, deposition ~ eruption	Eruption-volcanic-sedimentary
	Jurassic	Upper	Zhuanqiao Group	Upper	J_3z^3		150.1±0.9	152–303	Pyroxene trachyandesite with tuff breccia,tuff and Tuffite	
				Middle	J_3z^2			>400	Tuffite, tuffaceous sandstone, shale, usually alum petrochemical, kaolin-based	Volcanic-sedimentary
				Lower	J_3z^1			>530	Upper: gray-green trachyandesite, crystal dust tuff, tuffite; Central: lilac red breccia lava, sedimentary breccia tuff, tuff breccia, with muddy siltstone; Bottom: gray black breccia, sedimentary tuff breccia, sedimentary tuff, containing sedimentary pyrite, medium-thick layer of hematite	Extravasation-volcanic-sedimentary; Eruption-sedimentary
			Longmenyuan Group	Upper	J_3l^2			>290	Upper: yellowish brown mediate porphyritic hornblende andesite, thick layer of gray purple crystalline dust tuff; Lower: medium-fine porphyritic hornblende andesite, breccia lava and tuff lava, tuffaceous siltstone	Eruption-volcanic-sedimentary; Extravasation-volcanic-sedimentary
				Lower	J_3l^1		167	>150	Thick layer of purple andesitic volcanic breccia, fine porphyritic andesitic breccia lava	Eruption-extravasation
		Middle	Luoling Group	Upper	J_2l^2			>665	Limestone nodules containing siltstone, silty shale, and feldspathic sandstone	
				Lower	J_2l^1			1017	Siltstone, silty shale with feldspathic sandstone	
		Lower	Moshan Group	Upper	J_1m^2			374	Sandy shale, siltstone, shale, feldspathic sandstone with a small amount of thin coal seam	
					T_3J			63	Siltstone, mudstone, sandy shale, and carbonaceous shale	

Figure 3. The integrated stratigraphic column of the Luzong basin.

monzonite, respectively. The central phase was formed relatively a little later than the edge phase, but basically at the same time (Ren *et al*. 1991; Yang *et al*. 1993; Yang *et al*. 1996; Zhou *et al*. 2007). The SHRIMP zircon U-Pb age is 133.5 ± 0.6 Ma (Zhou *et al*. 2007), indicating that it formed in the Early Cretaceous.

Huangmeijian intrusion

The Huangmeijian A-type granite pluton is located at the SE margin of the Luzong volcanic basin with an exposure area of about 90 km^2 (Figure 2). Field geological surveys and petrological observations indicated that the Huangmeijian intrusive body is mainly composed of quartz syenite (pophyry) with a minor amount of biotite syenite and fine-grained granite. The LA-ICP-MS zircon U-Pb dating reveals the formation age for Huangmeijian intrusion is 125.4 ± 1.7 million years (Fan *et al*. 2008), or 127.1 ± 1.4 million years (Li *et al*. 2011) in the Early Cretaceous. Intrusion rocks exhibit obvious intrusive contact relationships with Jurassic wall-rocks, mainly feldspar quartz sandstone and trachyandesite volcanic rocks. Hydrothermal uranium mineralization found near the contact zone between the intrusion body and the sandstones demonstrated the existence of contact metasomatic phenomena in this region (Zhang *et al*. 1988).

Analytical method

We collected 15 samples from Shuangmiao Group, five samples from Bajiatan intrusion, and five samples from Huangmeijian intrusion in this study. Polished slices of samples were prepared and examined with a microscope to study petrology. Fresh fragments without weathering alteration were picked out from crushed whole-rock samples for chemical analyses.

Analyses of major elements were undertaken at the Mineral Laboratory of Aoshi in Guangzhou using a ME-XRF-06 by the melting film method, calibrated against international standards of appropriate compositions. Precision was determined from replicate analyses and is better than 1% for all major elements: SiO_2: 0.8%; Al_2O_3: 0.5%; Fe_2O_3: 0.4%; MgO: 0.4%; CaO: 0.6%; Na_2O: 0.3%; K_2O: 0.4%; MnO: 0.7%; TiO_2: 0.9%; and P_2O_5: 0.8%.

We employed the HNO_3 + HF seal dissolution method for trace elements and REE analyses by adding the Rh internal standard and converting the sample solutions into 1% HNO_3 medium. Eighteen trace elements were analysed by ICP-MS of ME-MS81-type. Accuracies of analyses of trace elements are determined as Ba: 2.7%; Ta: 2.1%; Nb: 1.6%; Zr: 2.2%; Hf: 2.1%; Th: 2.1%; U: 3.4%; Pb: 3.2%; Ga: 1.9%; Cr: 5.3%; Co: 0.8%; Ni: 11%; Cu: 3.5%; Rb: 2.1%; Sr: 1.7%; Sc: 4.2%; V: 3.2%; and Zn: 3.0%.

REE were determined by cation exchange separation–inductively coupled plasma atomic emission spectrometry with detection precisions of La: 4.7%; Ce: 5.2%; Pr: 1.8%; Sm: 4.7%; Eu: 1.2%; Gd: 1.4%; Tb: 3.2%; Dy: 4.3%; Ho: 2.4%; Er: 3.9%; Tm: 4.8%; Yb: 4.3%; Lu: 3.9%; and Y: 1.8%.

Petrography

Shuangmiao Group rocks

The rock samples from Shuangmiao Group are basaltic trachyandesite with grey-black massive structure and interwoven texture (Figure 4). These samples consist of ~70% matrix and ~30% phaneritic minerals as plagioclase and pyroxene. The majority of the plagioclase is andesine and the remaining is labradorite, with subhedral shape and various particle sizes ranging from 0.5 mm to 3.5 mm (Figure 4A and 4B). Some plagioclase is in dark marginal texture (Figure 4C) with clear carbonatation and silication phenomena. The slightly brown minerals with cleavages and xenomorphic textures that are filled in the space between plagioclase particles (Figure 4B and 4D) are augites, a type of pyroxene, with various particle sizes from 0.05 mm to 0.1 mm (Figure 4B–4D). The matrix is mainly weakly directional microcrystalline plagioclase, accompanying a small amount of volcanic glass and some aphanitic stuff.

Bajiatan intrusions

Bajiatan intrusive samples are all grey pyroxene monzonites with semi-euhedral medium- to coarse-granular texture and massive structure. These rocks are composed mainly of alkali-feldspar (35–40%), plagioclase (35–40%), pyroxene (10–15%), and biotite (2–3%) (Figure 5). Alkali-feldspar is mostly hypautomorphic granular in texture and localized irregular in shape, with various particle sizes 0.5–4 mm. Kaolinization of alkali feldspar is severe as revealed by the vague mineral surface (Figure 5A and 5B). Plagioclase is mostly euhedral-hypautomorphic tabular- to columnar-shaped, with minor sericitization and clay alteration as poly-film double-crystal and ring-band structure is still present for some grains (Figure 5A and 5B). Cleavage-developed multi-colourful biotite is mostly feuhedral-hypautomorphic sheet (Figure 5C and 5D). Pyroxene is mostly hypautomorphic-euhedral granular or columnar, with particle sizes 0.1–1 mm. Some pyroxene grains have grown simple double crystals. Weak chloritization exists due to the latter (Figure 5B and 5C). Deputy minerals are mainly magnetite, apatite, and sphene.

Huangmeijian intrusion

Fresh red Huangmeijian quartz syenite porphyry exhibits porphyriod texture and massive structure. More than 50% of its components are phenocrysts, mainly alkali

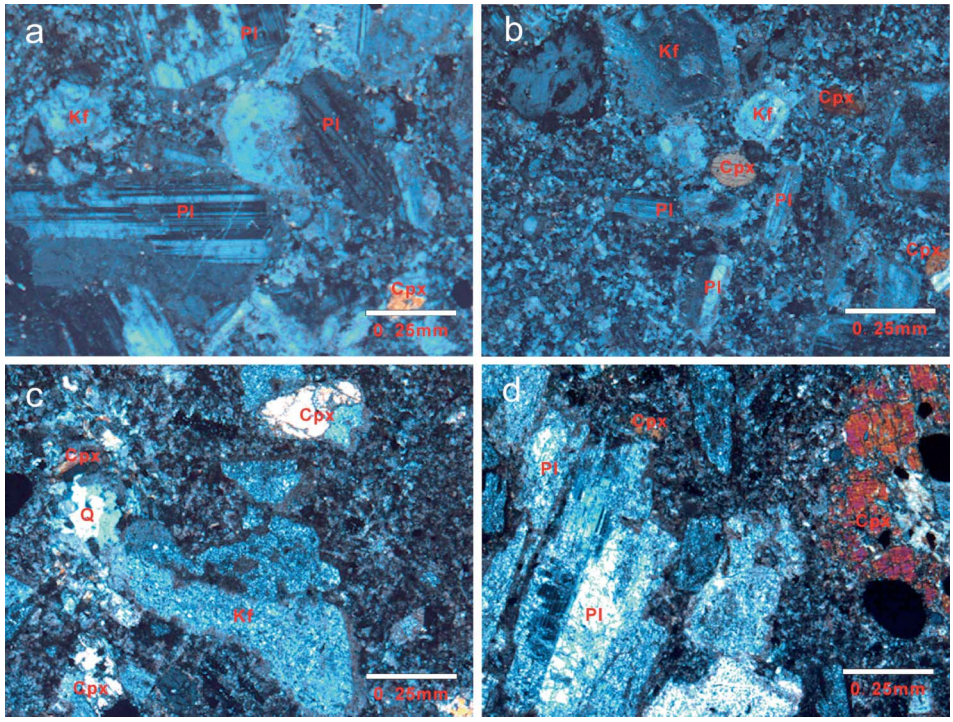

Figure 4. Shuangmiao Group (basaltic) trachyte andesite micrographs (orthogonal polarization). Note: Q, quartz; Cpx, clinopyroxene Kf, K-feldspar; Pl, plagioclase.

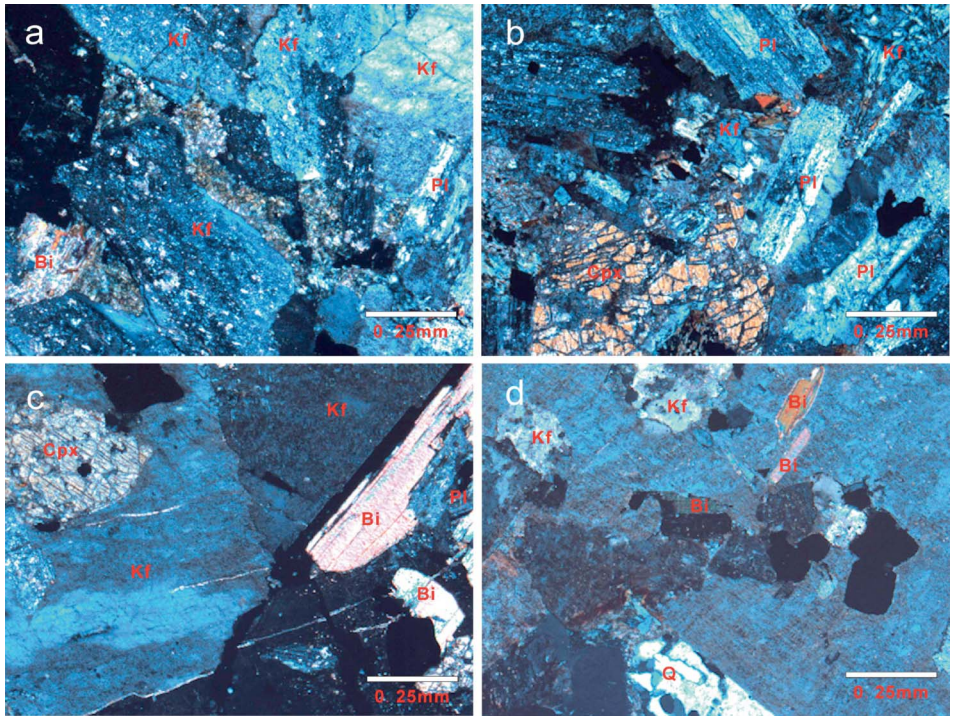

Figure 5. Bajiatan pyroxene monzonite micrographs (orthogonal polarization). Note: Q, quartz; Cpx, clinopyroxene; Kf, K-feldspar; Pl, plagioclase; Bi, biotite.

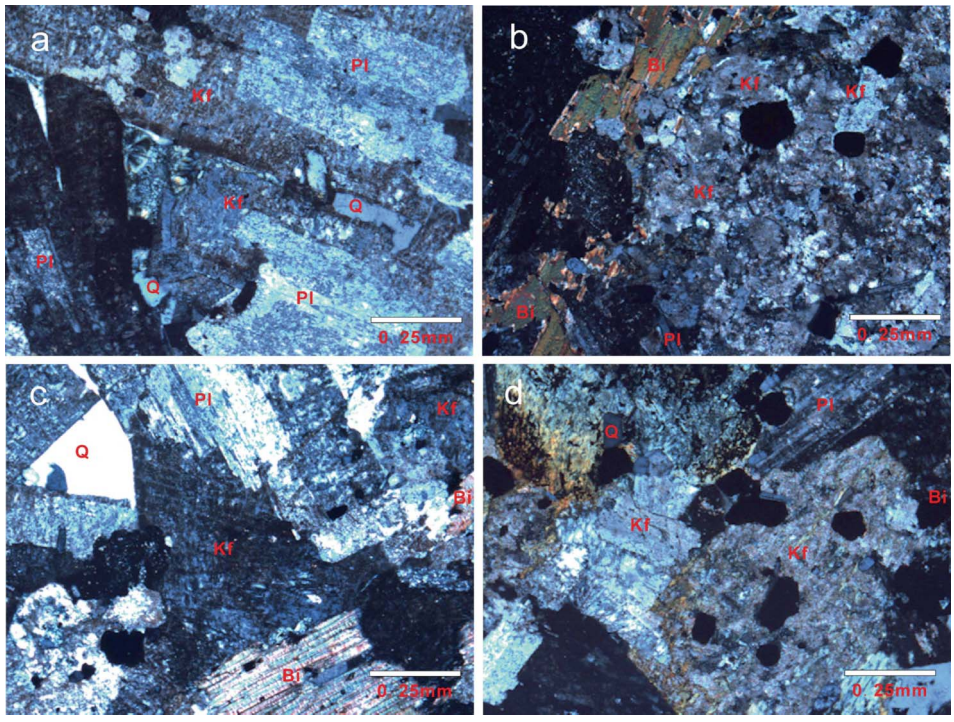

Figure 6. Huangmeijian quartz syenite micrographs (orthogonal polarization). Note: Q, quartz; Kf, K-feldspar; Pl, plagioclase; Bi, biotite.

feldspar, plagioclase, and biotite (Figure 6). Alkali feldspar phenocrysts are mostly euhedral-hypautomorphic columnar, and the particle size can be greater than 2 mm. Several alkali feldspar grains have grown casbah double-crystal (Figure 6A–D). Plagioclase phenocrysts are mostly tabular-columnar-shaped, and some poly-film double-crystals are observed (Figure 6A, 6Cand 6D). Both alkali feldspar and plagioclase phenocrysts show partial clayization. Biotite phenocrysts are mostly euhedral, flake, multi-colourful, with partial dissolution phenomena (Figure 6B and 6C). The matrix is in granular in texture, mainly composed of feldspar, quartz, and other minerals. Deputy minerals are mainly apatite, zircon, sphene, and magnetite.

Results and discussion

Tables 1 and 2 present analytical results of whole-rock major elements and trace (REE) elements for the total 25 samples of this study, respectively.

Major elements

Characteristics of major elements

Basaltic trachyandesites in the Shuangmiao Group contain middle-high SiO_2 contents ranging from 48.38 to 58.75% (average 55.49%; intermediate to mafic), while pyroxene monzonites from Bajiatan intrusion and quartz syenite porphyries from Huangmeijian intrusion exhibit SiO_2 contents of 49.04–54.89% (average 53.01%; intermediate to mafic) and 64.5–70.21% (average 65.20%; felsic), respectively (Table 1).

Alkali enrichment

Alkali enrichment is a common feature of volcanic rocks in Luzong basin. The total alkali contents ($K_2O + Na_2O$) of volcanic rocks from the Shuangmiao Group range from 6.12 to 10.47% with an average value of 8.08% (average $K_2O/Na_2O = 1.18$); Bajiatan intrusive rocks contain 8.18–8.79% of total alkali with an average of 8.47% (average $K_2O/Na_2O = 1.33$); for Huangmeijian intrusive rocks, total alkali contents cover a range from 9.32 to 11.55% with an average of 10.33% (average $K_2O/Na_2O = 1.16$).

Al-rich and poor in Ti

All analysed rock samples in the study area are enriched in Al_2O_3 and depleted in Ti. Al_2O_3 contents in all samples cover a range from 14.84 to 19.11% with an average value of 17.42%; TiO_2 contents cover a range of 0.19–1.25% with an average value of 0.80%.

High Fe_2O_3

Fe_2O_3 contents in samples from Shuangmiao Group and Bajiatan intrusion range from 5.48 to 9.15% (average 6.80%) and 7.43 to 8.96% (average 8.17%), respectively;

Table 1. Results of major elements of samples in the Luzong volcanic basin (wt.%).

Sample no.	Locality	Rock type	SiO_2	Al_2O_3	Fe_2O_3	CaO	MgO	Na_2O	K_2O	Cr_2O_3	TiO_2	MnO	P_2O_5	SrO	BaO	LOI	Total
SM-01	Shuangmiao	Basaltic trachyandesites	58.72	17.71	5.89	3.8	1.66	4.35	5.07	<0.01	0.71	0.17	0.328	0.11	0.09	0.63	99.23
SM-02	Shuangmiao	Basaltic trachyandesites	51.46	17.75	7.79	3.7	2.25	2.84	5.59	<0.01	0.93	0.14	0.481	0.04	0.06	5.68	98.71
SM-03	Shuangmiao	Basaltic trachyandesites	58.49	17.52	5.78	4.52	2.09	4.28	4.71	<0.01	0.61	0.21	0.328	0.11	0.07	0.74	99.45
SM-04	Shuangmiao	Basaltic trachyandesites	50.71	17.58	7.2	4.77	1.04	2.08	8.39	<0.01	0.89	0.21	0.481	0.02	0.14	5.88	99.39
SM-05	Shuangmiao	Basaltic trachyandesites	58.75	17.95	5.81	2.36	1.88	5.08	5.29	<0.01	0.6	0.1	0.327	0.08	0.08	1.58	99.89
SM-06	Shuangmiao	Basaltic trachyandesites	49.84	17.37	9.15	6.41	4.26	2.66	3.46	<0.01	1.03	0.12	0.508	0.09	0.06	4.63	99.59
SM-07	Shuangmiao	Basaltic trachyandesites	52.38	18.53	6.6	6.37	2.19	3.65	3.42	<0.01	0.95	0.16	0.495	0.1	0.06	4.33	99.24
SM-08	Shuangmiao	Basaltic trachyandesites	52.37	18.8	6.84	6.4	1.66	3.91	3.59	<0.01	0.97	0.15	0.487	0.1	0.07	4.33	99.67
SM-09	Shuangmiao	Basaltic trachyandesites	55.44	17.52	5.77	5.07	2.1	3.87	4.74	<0.01	0.72	0.16	0.36	0.11	0.06	4.03	99.95
SM-10	Shuangmiao	Basaltic trachyandesites	58.49	17.78	5.48	2.72	1.99	5.21	4.88	<0.01	0.6	0.12	0.33	0.08	0.07	1.76	99.52
SM-11	Shuangmiao	Basaltic trachyandesites	51.1	19.11	7.15	6.16	2.47	3.74	3.54	<0.01	0.96	0.18	0.51	0.1	0.07	4.62	99.7
SM-12	Shuangmiao	Basaltic trachyandesites	48.38	18.29	8.32	7.7	3.41	3.04	3.24	<0.01	1.08	0.12	0.534	0.1	0.07	5.39	99.67
SM-13	Shuangmiao	Basaltic trachyandesites	51.62	18.65	6.62	6.46	2.45	3.66	3.54	<0.01	0.93	0.17	0.496	0.11	0.07	4.69	99.46
SM-14	Shuangmiao	Basaltic trachyandesites	51.15	18	7.39	6.35	2.36	3.51	3.42	<0.01	0.89	0.16	0.483	0.1	0.07	4.81	98.69
SM-15	Shuangmiao	Basaltic trachyandesites	52.63	18.27	6.96	6.37	1.81	3.51	3.8	<0.01	0.91	0.16	0.485	0.09	0.06	4.67	99.72
HMJ-01	Huangmeijian	A-type granite	56.49	17.23	7.03	2.73	1.98	4.06	5.26	<0.01	0.92	0.15	0.417	0.05	0.07	3.34	99.73
HMJ-02	Huangmeijian	A-type granite	70.13	14.9	2.97	0.17	0.03	4.9	4.57	<0.01	0.2	0.02	0.023	<0.01	0.01	0.75	98.67
HMJ-03	Huangmeijian	A-type granite	70.21	14.84	3.57	0.36	0.03	4.89	4.73	<0.01	0.19	0.02	0.02	<0.01	0.01	1	99.87
HMJ-04	Huangmeijian	A-type granite	64.5	18.21	2.87	0.45	0.12	4.98	6.57	<0.01	0.52	0.16	0.099	0.01	0.03	1.24	99.75
HMJ-05	Huangmeijian	A-type granite	64.69	18.11	2.84	0.53	0.15	4.97	6.55	<0.01	0.47	0.09	0.092	0.01	0.02	1.47	99.99
BJT-02	Bajiatan	Pyroxene monzonite	52.05	16.65	8.45	3.69	3	4.07	4.72	<0.01	1.11	0.15	0.508	0.06	0.06	5.34	99.87
BJT-03	Bajiatan	Pyroxene monzonite	49.04	15.63	8.96	6.02	2.31	2.9	5.29	<0.01	1.25	0.18	0.62	0.04	0.07	6.58	98.9
BJT-04	Bajiatan	Pyroxene monzonite	54.24	16.88	7.89	4.18	2.82	3.8	4.71	<0.01	0.97	0.15	0.476	0.07	0.07	2.64	98.89
BJT-05	Bajiatan	Pyroxene monzonite	54.84	17.02	7.43	4.15	2.57	3.8	4.84	<0.01	1.02	0.13	0.469	0.07	0.07	2.72	99.13
BJT-06	Bajiatan	Pyroxene monzonite	54.89	17.38	8.12	4.87	2.78	3.58	4.6	<0.01	1.05	0.16	0.497	0.1	0.07	1.54	99.64

Table 2. Results of trace (REE) elements in the Luzong volcanic basin (ppm).

Sample no.	Ba	Ce	Co	Cr	Cs	Cu	Dy	Er	Eu	Ga	Gd	Hf	Ho	La	Lu	Mo	Nb	Nd
SM-01	783	109.5	14.3	10	5.36	50	3.97	2.35	1.62	23.2	6.06	9.7	0.78	57.6	0.39	4	29.9	40.1
SM-02	523	86	28.7	< 10	12.1	39	4.3	2.36	1.77	22	6.08	4.8	0.84	42.9	0.34	2	13.3	37.4
SM-03	621	113.5	15.1	10	6.38	76	4.09	2.42	1.66	23.1	6.35	9.7	0.81	60.4	0.4	3	30.8	41.7
SM-04	1240	84.4	14	< 10	5.89	45	4.09	2.29	1.69	20.9	5.97	4.8	0.81	41.8	0.34	2	13.2	37.2
SM-05	685	108	21.6	10	1.82	101	3.93	2.35	1.66	22.1	6.42	9.6	0.76	56	0.36	4	25.9	40.9
SM-06	470	77.4	27.2	10	2.23	21	3.99	2.22	1.86	20.1	6.21	3.8	0.78	37.7	0.29	2	9.2	36.1
SM-07	561	85.3	18	< 10	4.17	28	4.05	2.32	1.89	20.8	6.16	4.6	0.79	43.1	0.33	2	11.4	37.8
SM-08	558	84	19.7	< 10	5.56	25	3.92	2.26	1.8	20.8	6.03	4.6	0.75	42.4	0.32	2	11.4	37.2
SM-09	551	110.5	17.9	10	5.66	125	4.39	2.55	1.75	21.8	7.25	9.7	0.85	56.7	0.4	3	27.3	44.2
SM-10	592	100	11.8	< 10	1.65	38	3.81	2.22	1.58	21.1	6.29	9.1	0.74	52.6	0.36	2	24.3	38.5
SM-11	542	84.2	19.8	< 10	5.6	26	4.14	2.37	1.93	21.7	6.36	4.6	0.81	42.4	0.32	2	11.7	37.7
SM-12	528	80.8	24.6	10	2.78	244	4.31	2.38	2.04	21.3	6.83	4	0.83	39.9	0.32	2	9.7	37.9
SM-13	628	88.1	23.1	< 10	5.25	25	4.28	2.48	1.99	21.6	6.64	4.7	0.83	44.3	0.35	2	11.8	39.2
SM-14	559	86.3	23.1	< 10	5.43	34	4.1	2.35	1.93	21.5	6.39	4.6	0.8	43.3	0.32	2	11.5	38.2
SM-15	534	82.4	17.8	< 10	5.77	24	4.14	2.37	1.93	21	6.36	4.6	0.8	41.7	0.33	2	11.3	36.7
HMJ-01	584	99.9	15.4	10	3.71	51	4.37	2.55	1.59	20.8	6.66	8.8	0.82	50.5	0.38	4	19.1	41.7
HMJ-02	49.4	246	1.6	< 10	1.96	8	8.83	5.95	0.4	30.3	11.2	25.5	1.83	122.5	1.03	7	134.5	70.9
HMJ-03	59.9	288	2	10	1.49	7	7.24	5	0.35	30.1	10.6	22.2	1.53	138	0.92	5	151	71.6
HMJ-04	203	86.8	1.4	< 10	1.89	5	4.46	2.72	1.43	20.4	5.63	14.2	0.91	38	0.45	4	31.2	30.8
HMJ-05	185	93	1.4	< 10	1.79	5	4.78	2.84	1.65	20.6	6.56	13.5	0.95	49.7	0.47	3	29.9	39.1
BJT-02	567	107	18.8	10	5.88	66	4.69	2.62	1.72	20.9	7.38	6.1	0.91	53.5	0.37	5	18.7	45.7
BJT-03	607	115.5	23.6	10	3.86	116	5.3	2.92	1.7	21.2	8.24	6.4	1.02	55.3	0.41	5	18.5	51
BJT-04	591	105.5	19.7	10	4.92	74	4.57	2.61	1.73	21.4	7.08	6.8	0.91	52.7	0.37	4	18.7	44.1
BJT-05	596	103	18.2	10	4.93	70	4.47	2.62	1.77	20.6	7	7.2	0.87	51.9	0.37	4	19.3	43.1
BJT-06	575	106	19.8	10	3.5	90	4.53	2.6	1.76	21	7.02	7.1	0.88	54.1	0.37	5	18.7	44.1

(Continued)

Table 2. (Continued).

	Ni	Pb	Pr	Rb	Sm	Sn	Sr	Ta	Tb	Th	Tl	Tm	U	V	W	Y	Yb	Zn	Zr
SM-01	8	34	11.8	226	6.81	2	978	2.2	0.81	52.1	< 0.5	0.37	16.5	120	7	20.9	2.44	102	372
SM-02	< 5	36	10.1	190	6.5	1	327	0.9	0.83	13.55	0.6	0.34	3.93	181	3	21.4	2.24	540	172
SM-03	5	25	12.25	206	7.01	1	979	2.2	0.81	55.6	< 0.5	0.37	17.5	119	7	21.7	2.53	109	364
SM-04	< 5	34	9.83	254	6.8	1	189	0.8	0.81	13.3	0.8	0.33	3.71	173	3	20.7	2.19	138	171
SM-05	5	19	11.6	215	6.93	1	765	1.8	0.81	50.5	< 0.5	0.34	15.95	94	4	21	2.28	65	374
SM-06	15	17	9.39	130.5	6.79	1	840	0.6	0.83	11.35	< 0.5	0.3	3.01	189	1	20.6	2.01	90	137
SM-07	6	23	9.9	122.5	6.67	< 1	946	0.7	0.81	12.9	< 0.5	0.32	4.09	139	1	21	2.13	141	172
SM-08	< 5	25	9.88	123	6.67	1	854	0.7	0.78	12.85	< 0.5	0.31	3.97	137	1	20.3	2.06	169	172
SM-09	6	169	12.3	204	7.78	1	1030	1.9	0.9	51.6	< 0.5	0.38	15.9	116	10	23.3	2.56	229	381
SM-10	< 5	12	10.85	194.5	6.44	1	719	1.7	0.76	48.2	< 0.5	0.32	15.3	93	4	19.6	2.24	84	353
SM-11	5	20	9.86	127	6.66	1	887	0.7	0.85	13.45	< 0.5	0.33	3.79	153	1	21.2	2.24	205	177
SM-12	16	20	9.75	122	7.16	1	960	0.6	0.86	11.9	< 0.5	0.31	3.09	206	1	21.3	2.06	160	147
SM-13	6	20	10.35	128.5	7.07	1	1025	0.7	0.85	13.4	< 0.5	0.34	4.04	152	1	21.9	2.2	123	178
SM-14	5	22	9.99	126.5	6.69	1	948	0.7	0.84	13.25	< 0.5	0.32	4.13	191	1	21.3	2.24	113	174
SM-15	5	34	9.67	137.5	6.58	1	829	0.7	0.81	13.05	< 0.5	0.33	3.99	152	2	21	2.14	230	176
HMJ-01	7	120	11.45	219	7.08	1	475	1.2	0.86	24.8	0.5	0.34	6.43	123	11	22.6	2.53	474	359
HMJ-02	< 5	18	23.5	285	11.1	16	31.9	9.4	1.6	117	< 0.5	0.96	55.6	< 5	3	47.4	7.04	30	668
HMJ-03	< 5	18	24.7	276	10.55	15	30	7	1.4	114.5	< 0.5	0.8	55.5	< 5	2	40.1	5.86	35	594
HMJ-04	< 5	17	8.57	207	5.84	2	83.9	1.9	0.83	16.3	< 0.5	0.41	3.24	17	3	23.9	2.91	41	591
HMJ-05	< 5	19	11	202	7.21	2	93.5	1.8	0.93	17.35	< 0.5	0.42	3.16	16	3	25	3	44	556
BJT-02	10	56	12.35	188.5	8.16	1	546	1.2	0.94	23.1	< 0.5	0.37	7.06	150	4	23.9	2.45	232	221
BJT-03	12	321	13.45	204	9.07	1	397	1.2	1.06	23.6	< 0.5	0.41	6.97	189	5	27.3	2.71	538	237
BJT-04	9	30	12	191	7.75	1	670	1.2	0.91	26.1	< 0.5	0.37	7.85	144	3	23.6	2.54	113	252
BJT-05	8	36	11.8	193.5	7.62	1	655	1.2	0.9	27.6	< 0.5	0.36	7.49	139	3	22.9	2.44	116	266
BJT-06	10	31	11.95	200	7.65	1	870	1.3	0.91	26.4	< 0.5	0.36	8.72	142	3	23.3	2.46	130	262

for rocks from Huangmeijian alkaline intrusion, Fe_2O_3 contents are relatively lower, ranging from 2.84 to 3.57% (average 3.06%). The relatively more abundant Fe_2O_3 contents at the first two sites are likely related to the massive iron mineralization in the Luzong Basin, such as the Luohe and Nihe iron deposits (Chang *et al*. 1991).

MgO content

Volcanic rocks in Shuangmiao Group, Bajiatan intrusion, and Huangmeijian intrusion contain 1.04–4.06% (average 2.23%), 2.31–3.00% (average 2.67%), and 0.03–0.15% (average 0.08%) of MgO, respectively.

Rock series and rock-type discrimination

Most samples in this study fall in the context of alkali series in the TAS discrimination diagram (Figure 7A): volcanic rocks of Shuangmiao Group are mainly basaltic trachyandesite and trachyandesite; Bajiatan intrusive rocks are mainly monzodiorite and monzonite; and felsic Huangmeijian intrusive rocks fall in the context of syenite and granite. The K_2O–Si_2O diagram demonstrated that most of the studied samples are projected into the shoshonite series except two rocks from Huangmeijian intrusion (Figure 7B).

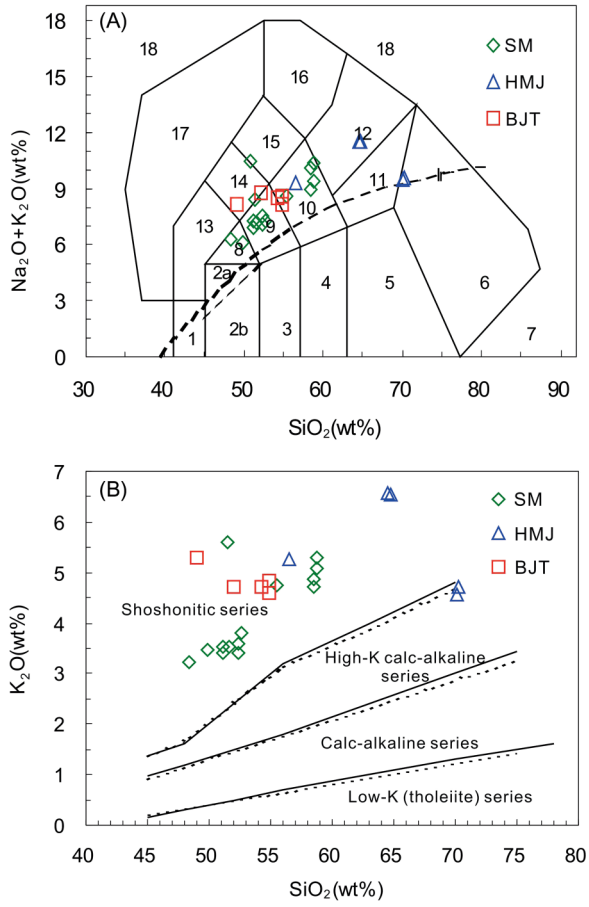

Figure 7. (A) TAS diagram of igneous rocks in Luzong (according to Middlemost, 1994). (B) K_2O–SiO_2 diagram of igneous rocks in Luzong. Note: Ir, Irvine dividing line, above is alkaline, below is sub-alkaline. SM, Shuangmiao Group; BJT, Bajiatan intrusion; HMJ, Huangmeijian A-type granite.
Plutonic: 1 – peridotite gabbro; 2a – alkaline gabbro; 2b – sub-alkaline gabbro; 3 – gabbro-diorite; 4 – diorite; 5 – granodiorite; 6 – granite; 7 – quartzolite; 8 – monzogabbro; 9 – monzodiorite; 10 – monzonite; 11 – quartz-monzonite; 12 – syenite; 13 – nepheline gabbro; 14 – nepheline monzodiorite; 15 – nepheline monzosyenite; 16 – nepheline syenite; 17 – foidolite; 18 – tawite/neapite/italite. Volcanic: 1 – picro-basalt; 2 – basalt; 3 – basaltic andesite; 4 – andesite; 5 – dacite; 6 – rhyolite; 7 – silicate-rich rock; 8 – trachybasalt; 9 – basaltic trachyandesite; 10 – trachyandesite; 11 – trachydacite; 12 – trachyte; 13 – tephrite; 14 – phonotephrite; 15 – tephriphonolite; 16 – phonolite; 17 – foidite; 18 – sodalitite/nephelinite/leucitite. *Solid line* is from Peccerillo and Taylor (1976), *dashed line* is from Middlemost (1985).

Trace elements

Volcanic rocks of the Shuangmiao Group

Samples from Shuangmiao Group show enrichments of Rb and Sr with Rb content from 122 ppm to 254 ppm (average 167 ppm) and Sr from 189 ppm to 1030 ppm (average 818 ppm), respectively. The Cr and Ni contents of Shuangmiao Group volcanic rocks are lower than 16 ppm, much lower than of the estimated abundance in the bulk silicate Earth (Cr and Ni content in primitive mantle are 300–500 ppm and 300–400 ppm, respectively). The chondrite-normalized spider diagram of trace elements (Figure 8) shows that Shuangmiao Group volcanic rocks show similar patterns with island-arc volcanic rocks, enriched in Rb, Sr, Ba, Cs, K, and other large-ion lithophile elements (LILEs). High field strength elements (HFSEs), such as U, Th, Zr, and Hf, show significantly positive anomalies. Ba and Sr behave similarly to alkali and Ca, respectively, as the main mineral carriers of Ba are K-feldspar and biotite, and of Sr are calcium–rich plagioclase and apatite.

The chondrite-normalized diagram (Figure 9A) of transition metal elements shows that Cr, Ni, and Co are strongly depleted compared with the crust, indicating that Cr, Ni, and Co probably resided in the magma source region in the form of chromite, olivine, and spinel during partial melting, which is an inherent characteristic of shoshonite series.

Nb contents of the 15 basaltic trachyandesite samples vary from 9.20 ppm to 30.80 ppm with an average value of 15.33 ppm, and Nb/Ta ratios cover a range of 13.59–16.85 with an average value of 15.47. In the spider diagram, the samples show Nb and Ta positive anomalies, similar to Nb-enriched basalts (NEBs) in eastern Mindanao, the Philippines (Nb contents are greater than 7 ppm; Sajona

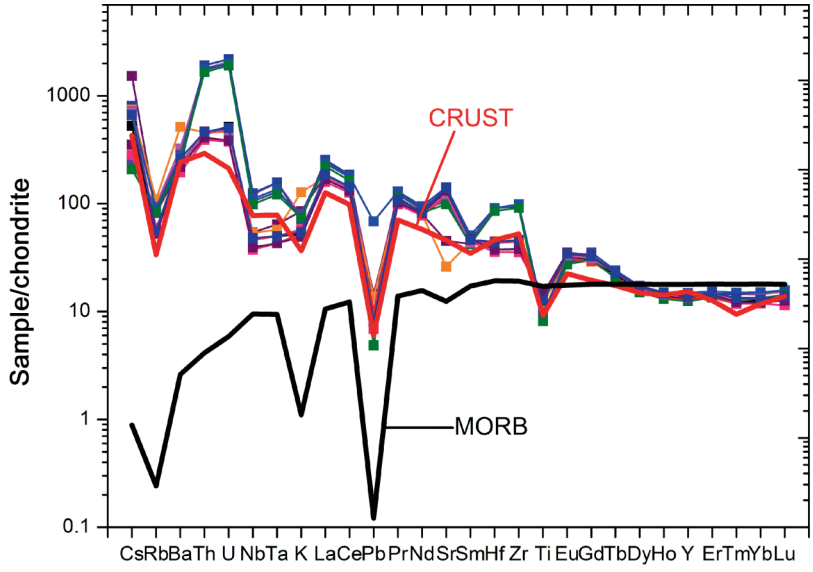

Figure 8. Trace elements spidergram of Shuangmiao Group volcanic rocks. Note: chondrite-normalized data are taken from Sun and McDonough (1989); crust and MORB values are from Hofmann (1988).

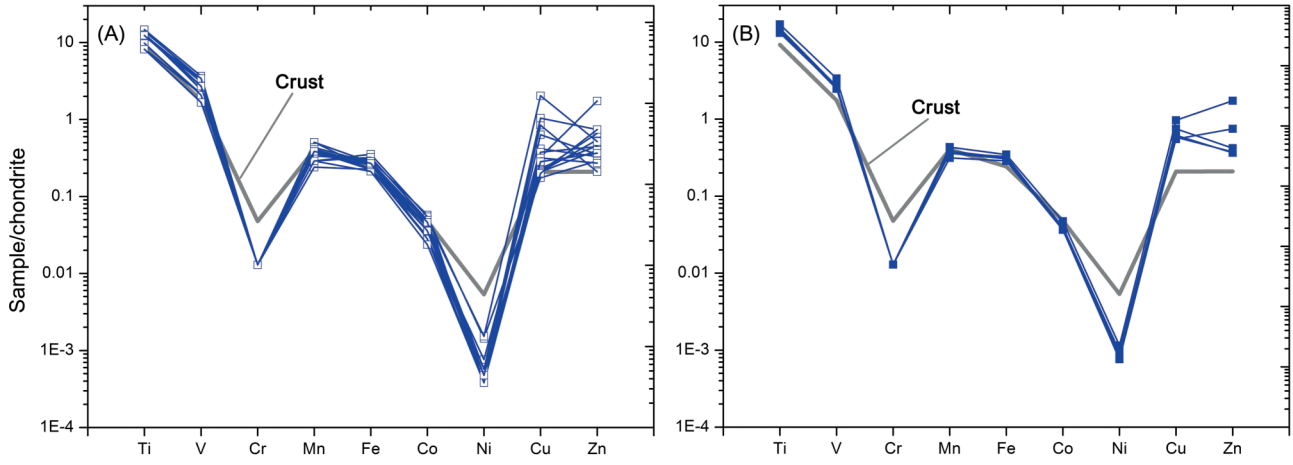

Figure 9. Transitional metal elements chondrite-normalized diagrams of Shuangmiao Group volcanic rocks (A) and Bajiatan intrusions (B). Note: chondrite-normalized data are taken from Sun and McDonough (1989); crust and MORB values are from Hofmann (1988).

et al. 1993, 1994). Reagan and Gill (1989) and Defant *et al*. (1991) once reported high-Nb basalts (HNBs; Nb contents are above 20 ppm), when they studied the arc-oceanic subduction system. The subsequent study found that part of the basaltic andesites formed by island-arc magma also had the same geochemical characteristics with NEBs, and therefore appropriately called them Nb-enriched basaltic andesite. It is likely that volcanic rocks in Shuangmiao Group are NEBs or HNBs (Figure 10). These NEBs have only been identified in the Pacific rim related to the oceanic plate subduction (Sajona *et al*. 1993; Kepezhinskas *et al*. 1996; Aguillón-Robles *et al*. 2001; Zhao *et al*. 2004; Zhang *et al*. 2005; Viruete *et al*. 2007; Calmus *et al*. 2008).

Bajiatan and Huangmeijian intrusions

The chondrite-normalized spider diagrams (Figure 11) illustrate that Bajiatan intrusive rocks are enriched in Rb, Sr, Ba, Cs, K, and other LILEs, and in contrast, Huangmeijian rocks are significantly depleted in Sr and Ba, which is the typical characteristic of A-type granites. For both sets of intrusive rocks, HFSEs such as U, Th, Zr, and Hf show significantly positive anomalies; Pb also shows significantly positive anomaly; Nb and Ta are slightly enriched; HREE are richer than the continental crust. Transition metal elements are distributed in the same pattern for all three studied sets of volcanic rocks (Figure 9B). Although Huangmeijian intrusive rocks exhibit some slightly different characteristics of trace

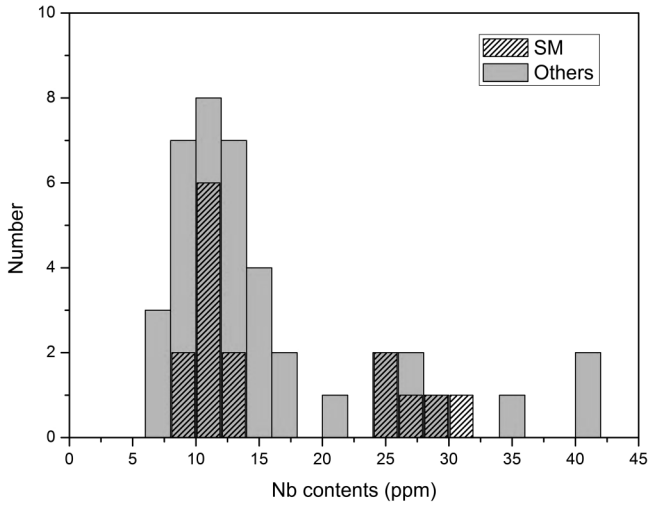

Figure 10. The statistical distribution of Nb contents of Shuangmiao Group volcanics and other NEB and HNBs. Note: SM, Shuangmiao Group volcanics; Others, NEB and HNBs of other region in the Pacific rim. Data are after Defant and Drummond (1993), Sajona *et al*. (1993, 1994, 1996), Aguilló-Robles *et al*. (2001), Viruete *et al*. (2007), Calmus *et al*. (2008), Dafant *et al*. (1992).

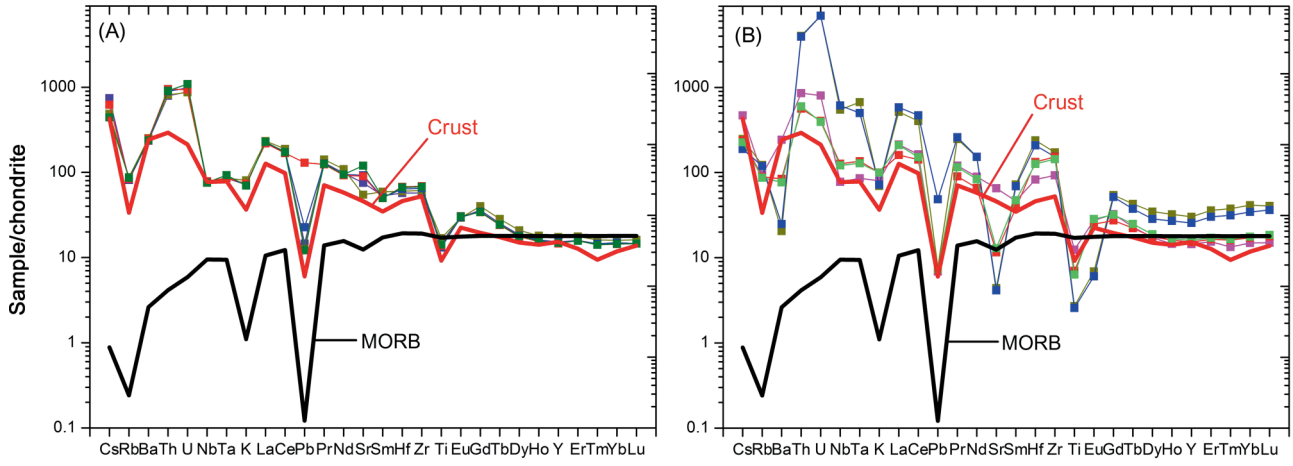

Figure 11. Trace elements spider gram of Bajiatan (A) and Huangmeijian (B) intrusions. Note: chondrite-normalized data are taken from Sun and McDonough (1989); crust and MORB values are from Hofmann (1988).

elements from rocks in the other two locations, they are still likely to be crystallized from the same original magma, since the Huangmeijian A-type granites were formed around 5–10 Ma later compared with the formation of Shuangmiao and Bajiatan igneous rocks, possibly as a result of magma evolution.

Volcanic rocks crystallized from melted crustal materials are normally poor in Ba, Sr and rich in Rb; in contrast, mantle-derived granites are enriched in Ba, Sr and depleted in Rb (Petford and Atherton 1996). Enrichment of Sr is a unique characteristic of potassium-rich rocks such as mantle-derived kimberlite, the crustal alkaline basalt, and olivine basalt (Xing and Xu 1995; Xing and Xu 1996), thus, our analytical results indicate that the magma source of the Luzong basin is likely derived from enriched mantle.

Rb/Sr and Rb/Ba ratios range from 0.12 to 1.34 and 0.20 to 0.37 for the igneous rocks from Shuangmiao Group and Bajiatan intrusion, respectively, which are much higher than the primitive mantle (0.029 and 0.088) (Sun and McDonough 1989), indicating that the magma had experienced a high degree of evolution and differentiation. Compared to the bulk continental crust, Luzong basin is enriched in LILEs and HFSEs. If the magma was only contaminated by the assimilation in the later evolution stage in the crust, it is impossible to form a more enriched rock than

the crust. The only possibility is that the magma came from a more enriched source.

Rare earth elements

Total REE contents (ΣREE) of Shuangmiao Group volcanic rocks range from 185.87 ppm to 254.30 ppm with an average of 214.10 ppm, with LREE/HREE ratio from 9.92 to 13.30 with an average of 11.33, δEu from 0.71 to 0.91 with average of 0.84, δCe from 1.00 to 1.04 with average of 1.02, La_N/Yb_N ratio from 13.45 to 17.62 with average of 14.95.

Bajiatan intrusive rocks exhibit ΣREE from 238.22 ppm to 268.09 p0pm (average 248.46 ppm), LREE/HREE ratio from 11.15 to 11.79 (average 11.52), δEu from 0.60 to 0.74 (average 0.69), δCe from 1.02 to 1.04 (average 1.03), La_N/Yb_N ratio from 14.64 to 15.77 (average 15.24).

The ΣREE of Huangmeijian intrusive rocks range from 189.76 ppm to 566.55 ppm (average 344.30 ppm), with LREE/HREE ratios from 9.36 to 15.99 (average 11.85), δEu from 0.10 to 0.76 (average 0.48, Eu-negative anomaly is obvious), δCe from 0.98 to 1.21 (average 1.10), La_N/Yb_N ratio from 9.37 to 16.89 (average 12.99).

The chondrite-normalized REE distribution patterns (Figure 12) illustrate that volcanic rocks in Luzong basin are characterized by enrichment in LREE and depletion in HREE. Slightly Eu-negative anomalies of Shuangmiao and Bajiatan igneous rocks indicate a weak fractionation of plagioclase during crystallization. Two samples of Huangmeijian intrusive rocks show strong Eu-negative anomalies, which may be related to the later formation of this intrusion body and strong differentiation during crystallization. SHRIMP zircon U-Pb dating demonstrated that the formation age of Bajiatan intrusion is 133 Ma (Zhou *et al*. 2007), of Shuangmiao Group is 130 Ma (Zhou *et al*. 2008), and of Huangmeijian intrusion is around 125 Ma (Fan *et al*. 2008), respectively. The formation ages of the studied three sets of volcanic rocks constrain the evolution sequences of igneous series in the Luzong basin.

The enrichment of LREE relative to HREE for all the three sets of igneous rocks is significantly different from the REE distribution pattern in normal mantle-derived rocks (e.g. MORB), which should usually be enriched in HREE. This indicates that the magma sources of Luzong basin are not derived from normal primitive mantle or depleted asthenospheric mantle, but mostly from the lithospheric mantle.

Sr–Nd isotope compositions

The Middle-Lower Yangtze polymetallic belt is located at the boundary between two regions with different mantle sources (Chung 1999). The North China block is characterized by an EMI-type enriched mantle source (Jahn *et al*. 1999), whereas the South China block is characterized by an EMII-type enriched mantle source (Chen and Jahn 1998). Employing Sr–Nd data of previous studies at Luzong basin, I_{Sr} values range from 0.70511 to 0.70726 and $\varepsilon_{Nd}(t)$ values range from −10.0 to −3.2 (Chen *et al*. 1993; Chen and Jahn 1998). The I_{Sr}-$\varepsilon_{Nd}(t)$ diagram shows that Sr–Nd composition of Luzong igneous rocks is probably derived from a magma source between the MORB and EM II end members (more close to EMII end member). Thus, we postulate that the magma source of Luzong volcanic basin was derived from an EMII-enriched mantle reservoir with possibly added components of soceanic slab materials (Figure 13). An alternative explanation is that the magma source was attributed to the slab roll-back of subducting Pacific plate (e.g. Wong *et al*. 2009) or a ridge subduction (Ling *et al*. 2009) based on the evolution history of the Pacific plate (Sun *et al*. 2007).

Tectonic setting discriminations

Bajiatan intrusive rocks

Pearce *et al*. (1984) performed the first systematic study over the geochemistry characteristics of granites with known tectonic settings. They generally defined intrusive rocks whose quartz contents were more than 5% as granitic rocks, and divided granites into four categories: ocean ridge granite (ORG), volcanic-arc granite (VAG), within-plate granite (WPG), and syn-collision granite (Syn-COLG). Employing Rb-Y-Nb and Rb-Yb-Ta tectonic setting discrimination diagrams, we could determine the tectonic environment of Bajiatan intrusion. Bajiatan intrusive rocks are mainly distributed at the junction area of VAG, Syn-COLG, and WPG, with obvious inclination to VAG field (Figure 14). Through the Hf+Rb/10+3Ta triangular diagram, we could distinguish ORG, VAG, and WPG more accurately (Figure 15). Because Syn-COLG is located in the joint field of VCG and WPG (Harris *et al*. 1986), zoomed Hf+Rb/30+3Ta diagram (Figure 15B) is used to expand the distribution field of Syn-COLG in order to make this special type of granite easier to be identified. Overall, it is clearly shown that Bajiatan intrusive rocks are formed in a volcanic arc tectonic setting (Figure 15A and 15B).

Huangmeijian intrusive rocks

Major trace elements and REE characteristics of Huangmeijian intrusive rocks indicate that they are typical A-type granites: rich in silicon and alkali, poor in calcium and magnesium (similar to S-Type, different from M-type because M-type granites usually have relatively high calcium, high sodium, low potassium, and no Eu anomalies), highly enriched HFSE (Nb, Zr, Y, and Ga), and depleted Sr and Ba (i.e. the significant difference from the other two types of granites), unusually high ∑REE and typical right-wing gull-type REE distribution patterns

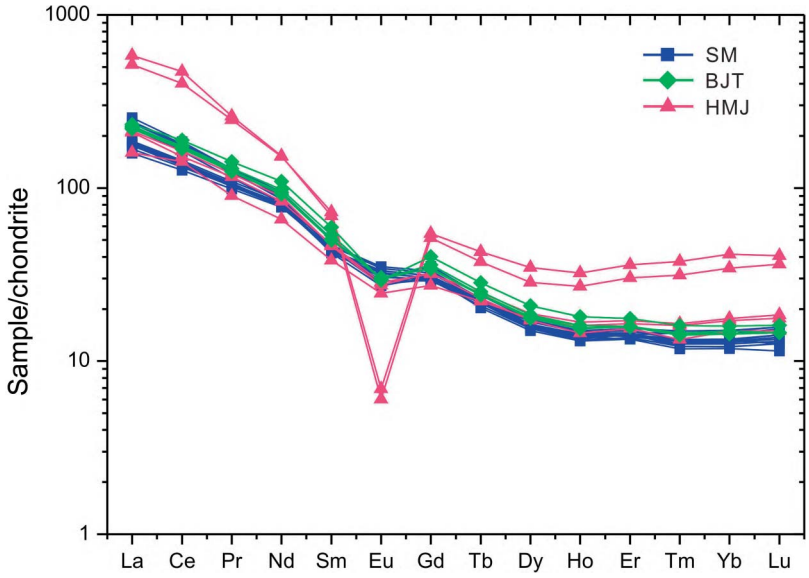

Figure 12. Chondrite-normalized REE distribution patterns of Shuangmiao Group volcanic rocks, Bajiatan and Huangmeijian intrusive rocks. Note: SM, Shuangmiao Group; BJT, Bajiatan intrusion; HMJ, Huangmeijian A-type granite. Chondrite-normalized data are taken from Sun and McDonough (1989).

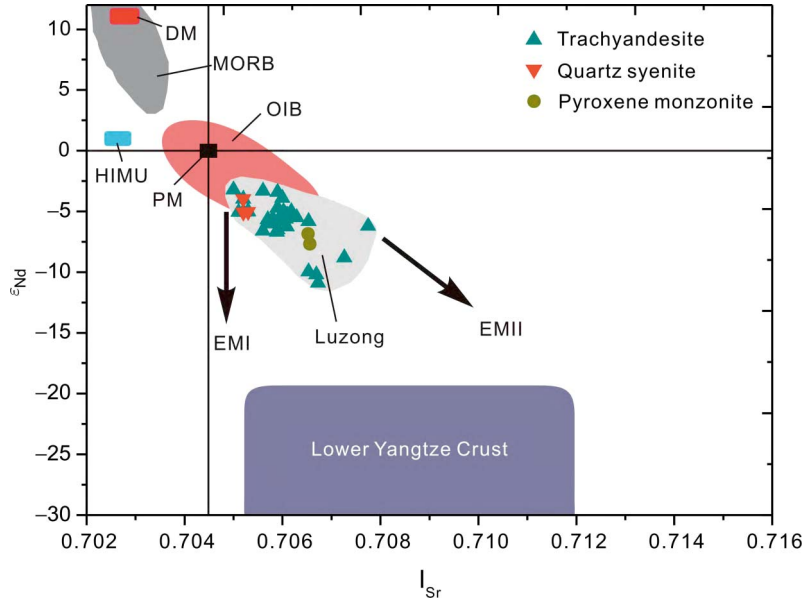

Figure 13. I_{Sr}-Nd(t) diagram of Luzong igneous rocks (after Zindler and Hart, 1986). Note: MORB, mid-ocean ridge basalt; OIB, ocean island basalt; EM(I, II), enriched mantle components; DM, depleted mantle components; PM, primitive mantle components; HIMU, high mantle components; Luzong, Sr–Nd isotope distribution area of Luzong igneous rocks.
The Sr–Nd data of trachyandesite are from Liu *et al.* (2002); Wang *et al*. (2006, 2003, 2001); Xie *et al*. (2007); Xing and Xu (1998); Yuan *et al.* (2008); Zhao *et al*. (2003); data of quartz-syenite are from Zhao *et al*. (2003); data of Pyroxene mozonite are from Ren *et al*. (1991).

(obvious Eu-negative anomalies). The trace element discrimination diagrams (Figure 16) also showed that they are A-type granites.

A-type granite was once a term proposed by Loiselle and Wones (1979) particularly for granites that represent an extensional setting, which geochemically are characterized by high absolute alkali abundance and very low H_2O content (Collins *et al*. 1982; Whalen *et al*. 1987). It is generally accepted that A-type granites are formed in an extensional tectonic setting (Eby 1992; Wang *et al*. 1995).

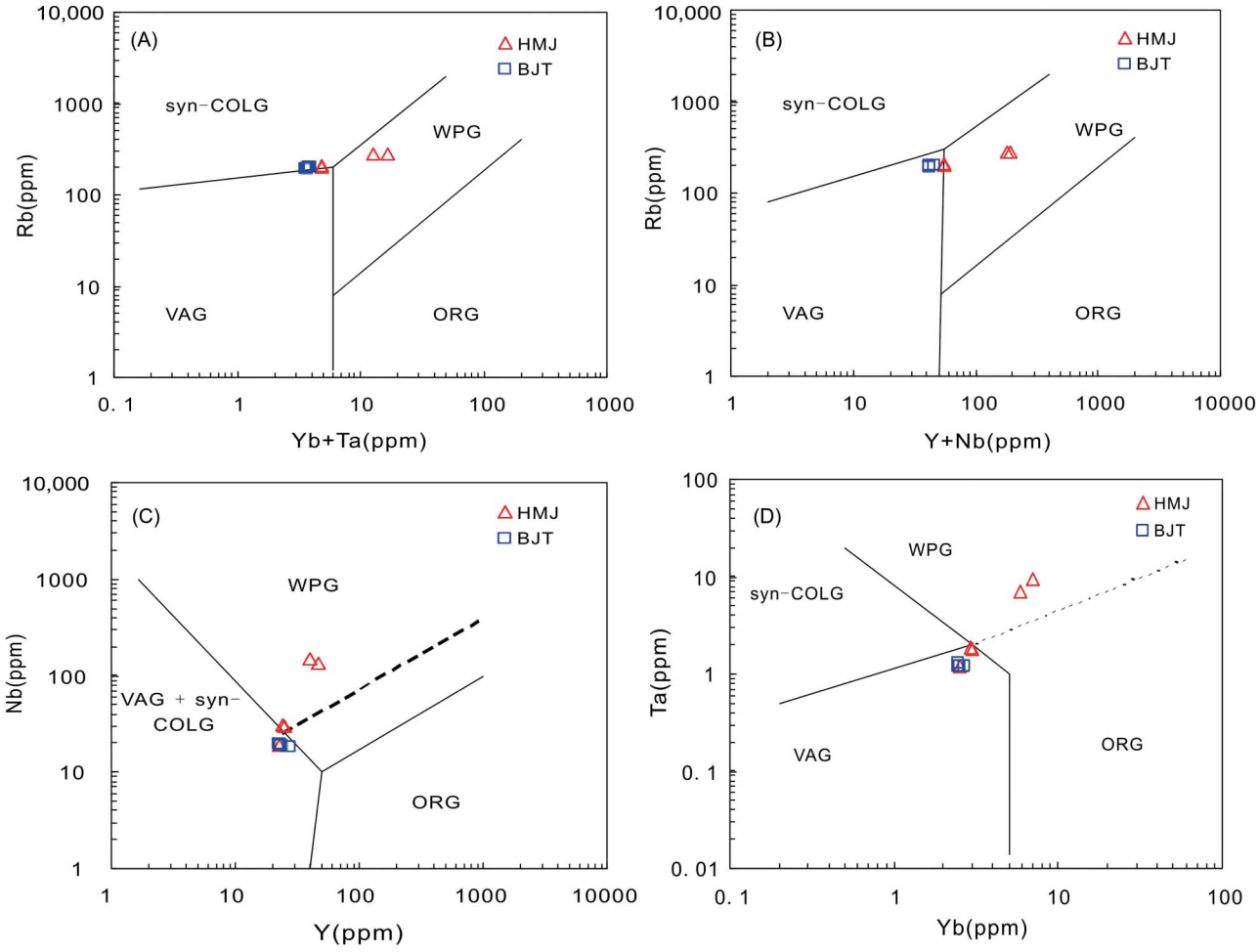

Figure 14. Tectonic discrimination diagrams of Bajiatan and Huangmeijian intrusions (after Pearce *et al*. 1984). (A) Rb–(Y + Ta) discrimination diagram; (B) Rb–(Y + Nb) discrimination diagram; (C) Nb–Y discrimination diagram; (D) Ta–Yb discrimination diagram. Note: VAG, volcanic-arc granite; Syn-COLG, syn-collision granite; WPG, within-plate granite; ORG, ocean ridge granite; Dashed line arises from the boundary line abnormal ridges ORG; BJT, Bajiatan intrusion; HMJ, Huangmeijian A-type granite.

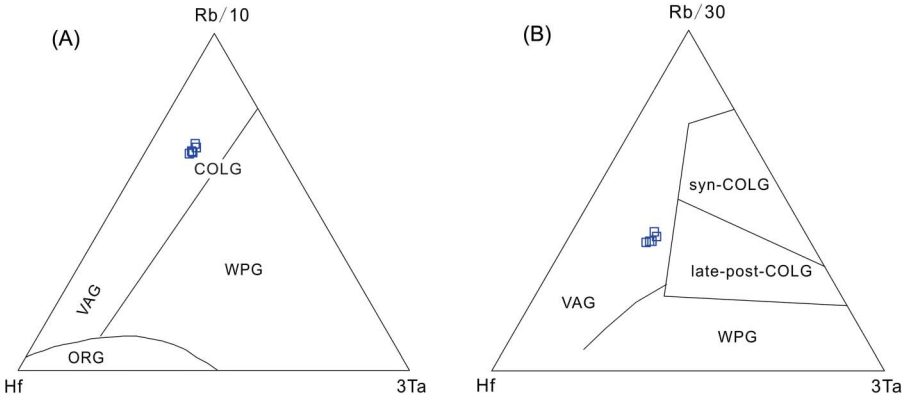

Figure 15. Hf-Rb-Ta tectonic discrimination diagrams of Bajiatan intrusion (after Harris *et al*. 1986). (A) Hf-Rb/10-3Ta discrimination diagrams of Bajiatan intrusions; (B) Hf-Rb/30-3Ta discrimination diagrams of Bajiatan intrusions. Note: VAG, volcanic-arc granite; COLG, collision granite; Syn-COLG, syn-collision granite; Late-post-COLG, late-post-collision granite; WPG, within-plate granite; ORG, ocean ridge granite.

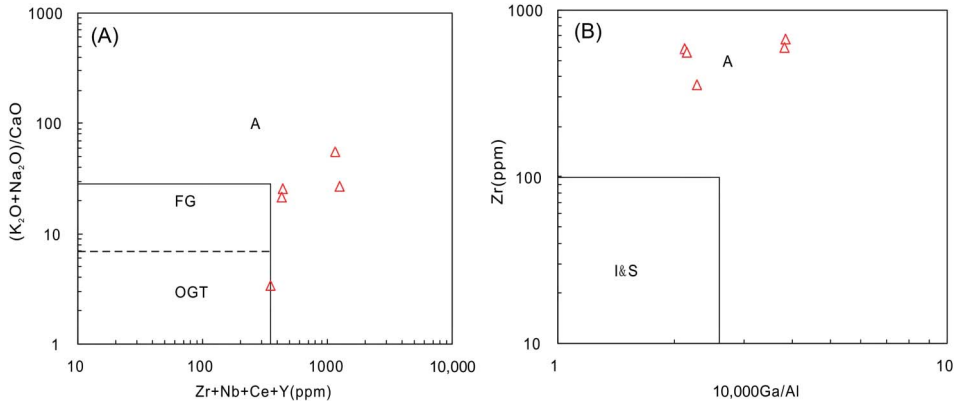

Figure 16. A-type granite classification diagram of Huangmeijian intrusion (after Whalen *et al*. 1987). (A) (K_2O+Na_2O)/CaO+Nb+Ce+Y classification diagram; (B) Zr-Ga/Al classification diagram. Note: A, A-type granites; FG, differentiated M+I+S-type granites; OGT, non-differentiated M+I+S-type granites; I&S, I- and S-type granites.

Eby (1992) divided A-type granites into two subclasses: A1 and A2 types. The distributions of compatible elements such as Rb, Ce, Y, Nb, Sc, Zr, Hf, Ta, and Ga of A1-type granites are similar to oceanic island basalts, indicating mantle-derived mantle sources (which can have a certain degree of crustal contamination) for the formation of A1-type granites. For A2-type granites, the distribution of these compatible elements is similar to various rocks from continental crustal rocks to island-arc basalts, demonstrating that the diagenetic substances are mainly derived from sedimentary but not metamorphic crustal source rocks. Volatile- and HFSE-bearing fluid may accumulate during the evolution of A-type granites and influence the crystallization of accessory minerals (Bonin *et al*. 1998). Further discrimination shows that the Huangmeijian intrusion is A1-type granite (Figure 17), indicating an enriched mantle magma source.

Volcanic rocks in the Shuangmiao Group

Tectonic discrimination diagrams of volcanic rocks in the Shuangmiao Group are shown in Figure 18. These diagrams show that all the samples concentrate in the field of volcanic-arc calc-alkaline basalt, indicating that these rocks were possibly formed in a tectonic setting similar to volcanic-arc related to a subduction zone.

Forming mechanism of the shoshonite series

Some scholars proposed that K- and Al-rich shoshonitic magma was formed at the depth of 100–175 km in the upper mantle, and generated by low degrees of partial melting (2–3%) of phlogopite-bearing garnet lherzolites in the Nanjing-Wuhu area (Xue and Tao 1989); their geochemical characteristics have total coincidence with those standards of Morrison (1980). Wang *et al*. (1991) once discussed the genesis of the shoshonitic rock series in Nanjing-Wuhu region and Luzong volcanic basin and proposed the concept of 'Shoshonite Province'. Most igneous rocks in the Luzong area are shoshonitic rocks, and some belong to calc-alkaline sub-series.

Two different tectonic settings have been proposed for shoshonitic rocks in the world. One common tectonic setting is related to the subduction zone (Condie

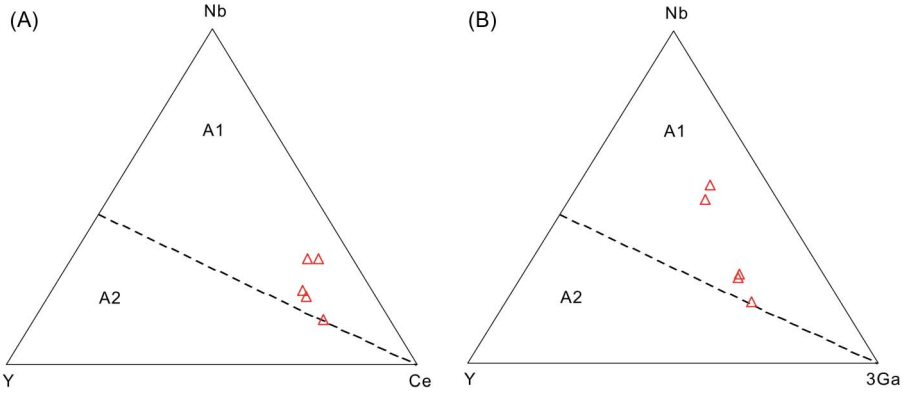

Figure 17. A-type granites subtypes (A1, A2) classification diagrams (according to Eby 1992). Note: A1 anorogenic granites; A2 post-orogenic A-type granites.

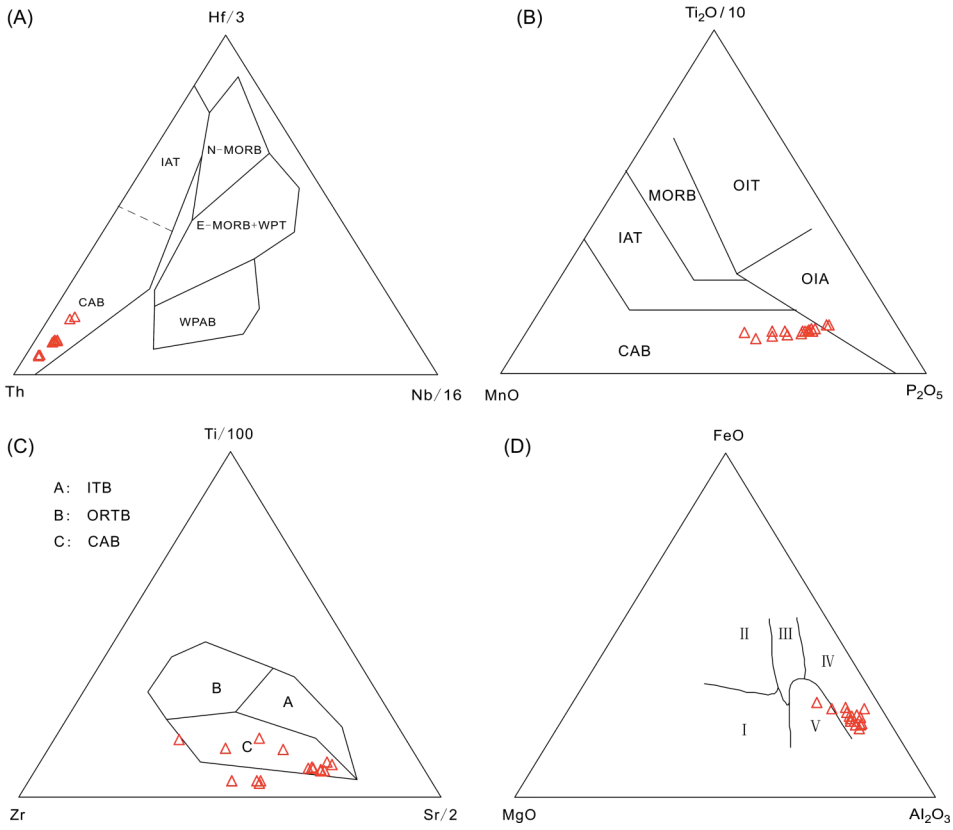

Figure 18. Tectonic environmental discriminations of Luzong volcanic rocks. (A) Th-Hf-Nb discrimination diagram of Shuangmiao Group volcanic rocks (according to Wood 1980) (CAB, volcanic arc calc-alkaline basalt; WPAB, within-plate alkaline basalt; WPT, within-plate tholeiite; IAT, island-arc tholeiite; *line* segments indicate the transition of different types of basalt). (B) Mn-TiO_2-P_2O_5 discrimination diagram of Shuangmiao Group volcanic rocks (according to Mullen 1983) (OIT, oceanic island tholeiite; OIA, ocean island alkaline basalt; MORB, mid-ocean ridge basalt; IAT, island-arc tholeiite; CAB, volcanic arc calc-alkaline basalt). (C) Ti-Zr-Sr discrimination diagram of Shuangmiao Group volcanic rocks (according to Pearce and Cann 1973) (A – island-arc basalt; B – calc-alkaline basalt; C – island-arc calc-alkaline basalt). (D) MgO-FeO(total)-Al_2O_3 diagram of Shuangmiao Group volcanic rocks (according to Pearce *et al*. 1977) (I – mid-ocean ridge or ocean floor; II – oceanic island; III – continent; IV – expansional central island volcanic arc calc-alkaline basalt; V – orogenic belt).

1982), and shoshonite or high-K trachyandesite are the most abundant components, which are mainly formed in an island-arc environment (Morrison 1980; Muller and Groves 1995). The other tectonic setting is in the intraplate rift and continental margin environments. The distributions of shoshonitic rocks formed in such environments are relatively less in the world.

Luzong volcanic basin is in the north of the Yangtze River, far away from Jiang-Shao fracture, the boundary of Yangtze-China plate. It is located at the south margin of Yangtze and North China craton boundary (Li 1994), and east of the Tan-Lu fault. Generally, Luzong basin is in the Yangtze Block intraplate environment. However, recent studies have shown that the Mesozoic palaeo-Pacific plate subduction to the Eurasian plate led subducted oceanic crust reaching so far to the Yangtze River region, and heavily impacted the magmatic activities. Thus, the tectonic setting of Luzong volcanic basin cannot be divorced from the Pacific plate subduction, and simply regarded as an intraplate environment. Tectonic setting discrimination diagrams of studied igneous rocks in the basin have shown they were formed in a volcanic-arc environment, possibly impacted by plate subduction. Major trace elements, REE, and other geochemistry characteristics indicate that the magma sources of this volcanic basin were derived from enriched mantle with added crustal components. Thus, palaeo-Pacific plate subduction to the Eurasian plate at Mesozoic time could be the main dynamic process that constrained the volcanic rocks in the Luzong basin; this point of view has also been supported by some other scholars (Wu and Qi 1985; Deng *et al*. 1996).

Chemical compositions and $^{87}Sr/^{86}Sr$ initial ratios of the shoshonitic rocks are similar to the high-K calc-alkaline series. With similar SiO_2 contents, the shoshonite is more enriched in alkali and relevant elements as Cr, Ni, Co, Sr, Ba, La, Ce, and La/Y ratios (Condie 1982). The shoshonitic magma could be generated through some degrees of partial melting of any mantle source with contaminations from crustal rocks. Phase equilibrium correlation (Wang *et al*. 1991) could lead the shoshonitic

magma to be highly rich in K. There is no independent shoshonitic magma, and shoshonitic rock series in the Luzong basin is the product of magmatic evolution derived from enriched mantle sources, as supported by Sr–Nd isotope (Figure 13).

Xu and Zhu (1994) and Zhu *et al*. (2003) proposed that the oblique subduction of the palaeo-Pacific plate not only led to the left-translation of Tan-Lu fault during Early Cretaceous but also led to magmatic activities in the same period, just similar to the oblique subduction of the Farallon plate in the western North America during the Late Cretaceous to Palaeogene. Therefore, the magmatic activities that caused the mineralization of Cu, Au, and other metal deposits in the Middle-Lower Yangtze River region should be attributed to high-speed oblique subduction of palaeo-Pacific plate in the Early Cretaceous (about 140 Ma) (Engebretson *et al*. 1985; Maruyama *et al*. 1997; Sun *et al*. 2007). The Late Cretaceous (about 130 Ma) subducting plate steepened, inducing orogenic collapse and back-arc extension and resulting in the formation of highly K-rich volcanic rocks and A-type granites (Wang *et al*. 2004).

Pacific plate subduction also provides a reasonable explanation for the enriched magma sources of shoshonite in the Luzong basin. Along with the palaeo-Pacific plate subduction, deep-sea sediments and oceanic crust could be brought into the mantle with the subducting slab, and consequently dehydration and metasomatism occurred when fluid flew up to the overlying mantle wedge and formed the enriched magma through partial melting.

Nb-rich characteristics of igneous rocks also support the palaeo-Pacific-plate-subduction-related formation mechanism in Luzong basin. How NEBs or basaltic andesites are formed is still under debate. One proposal is that metasomatism of mantle peridotites by adakitic fluid caused partial melting of mantle and produced NEBs in an island-arc environment. However, adakites were formed by partial melting of subducting oceanic crust with existence of rutile (Sajona *et al*. 1993; Kepezhinskas *et al*. 1996; Viruete *et al*. 2007). Since Nb and Ta are heavily enriched in rutile, the formed adakitic fluid has obvious Nb- and Ta-negative anomalies, thus the lower crust is heavily depleted in Nb (Rudnick and Fountain 1995; Rudnick and Gao 2003). Adakites formed by lower-crust delamination should not be enriched in Nb, and could generate Nb-enriched basaltic sources by metasomatism. So we could abandon the point of view that lower-crust delamination can produce NEBs.

Another suggestion is that NEBs could be formed by partial melting of the debris left by the partial melting of subducting slab (Thorkelson and Breitsprecher 2005). This mechanism well explains the Nb enrichments of NEBs since debris' partial melting could lead upwelling of Nb-enriched magma to asthenoshpher; however, the debris produced by partial melting is often difficult to be re-melted in the absence of water, that is, whether partial melting could occur needs to be verified; on the other hand, when rutiles are present, Nb/Ta fractionation will occur during partial melting of subducting slab, causing the generated magma has a higher Nb/Ta ratio than the residual phase: it does not match with the fact that NEBs have a lower Nb/Ta value ($\sim$15.47, lower than the average value of MORB $\sim$17).

The theory of oceanic ridge subduction could better explain the Nb-rich characteristics of Early Cretaceous to Mesozoic igneous rocks in Luzong basin. Oceanic ridge subduction is the combination setting of subduction zone and ocean floor expansion (Thorkelson 1996), and was first identified during orogenic research in the western USA (Palmer 1968). Previous studies show that about 125 million years ago, the Pacific plate subducted to the SW direction, while the Izanagi plate subducted to the N and NW direction even faster (Maruyama *et al*. 1997; Sun *et al*. 2007). The oceanic ridge between the two plates was just opposite to Eurasia (Sun *et al*. 2007), and an oceanic ridge subduction setting was likely there (Ling *et al*. 2009). Oceanic ridge subduction may sometimes produce a slab window, release heat through physical and chemical interactions with the surrounding asthenosphere mantle, and change the structure and magmatic evolution of the overlying plate (Thorkelson 1996; Whittaker *et al*. 2007). The formation of a slab window has an important role in constraining the magma evolution of the corresponding region. According to the drifting histories of the Pacific and Izanagi plates (Maruyama *et al*. 1997) and other studies (Sun *et al*. 2007), we speculate that oceanic ridge subduction probably reached the Yangtze River region at about 125–145 Ma (existing studies showed the formation ages of the three types of magmatic rocks in Luzong region as following: Bajiatan intrusion, 133.5 $\pm$ 0.6 million years (Zhou *et al*. 2007); Shuangmiao Group, 130.5 $\pm$ 0.8 million years (Zhou *et al*. 2008); Huangmeijian A-type granites, 125.4 $\pm$ 1.7 million years (Fan *et al*. 2008).), and might have formed a slab window to generate the Yangtze River metallogenic belt and associated rocks. The high-Nb and low-Nb/Ta characteristics of NEBs may be caused by partial melting of a shallow mantle wedge in the slab window (Aguillón-Robles *et al*. 2001; Castillo 2008). Experimental and field studies of UHP rocks in the subduction zone show that Nb, Ta, and other HFSEs are active in the early dehydration process under pressure less than 1.5 GPa, before the conversion of blueschist facies to amphibole-bearing eclogite facies during subduction (Xiao *et al*. 2006; Ding *et al*. 2007), and these elements would likely to concentrate in the fluid phase. As the partial melting residue left in the source area, amphibole is more enriched in Nb than Ta, the fluids generated by dehydration of the subducting slab are characterized by low Nb/Ta ratios. The dehydration-generated fluids were then mixed with magma

from the partially melted subducting plate and subjected to a series of complex processes (Xiao *et al*. 2006). The shallow mantle wedge at subduction zones stores most Nb, Ta, and other incompatible elements at low temperature, but it is not likely to partially melt the mantle wedge and release Nb and Ta under low pressure in normal subduction zone conditions. However, due to the formation of the slab window and unloading of asthenosphere in a oceanic ridge subduction setting, upwelled hot fluid would make the water-bearing mantle wedge partially melted at a lower pressure and generate an enriched magma source for the formation of NEBs.

The oceanic ridge subduction model can well explain the high Nb content and relatively low Nb/Ta ratio of NEBs in Luzong basin, and it is also a very good explanation for the enriched features of magma sources where these rocks were derived.

Conclusion

(1) Early Cretaceous igneous rocks in the Luzong volcanic basin belong to the shoshonitic series. They formed in an extensional volcanic-arc environment reflecting subduction of the palaeo-Pacific plate beneath Eurasia. The existence of the NEBs in the basin firmly supports the influence of Pacific plate underflow.

(2) Oceanic ridge subduction led to the unloading and upwelling of asthenospheric mantle, which provided the necessary heat for the partial melting of an enriched mantle wedge. Igneous rocks in the Luzong basin were generated from enriched magma sources, the latter metasomatized by enriched fluids sourced from the dehydrating subducting oceanic crust and the partially melted overlying lithospheric mantle.

Acknowledgments

This study was supported by the National Natural Science Foundation of China (Nos. 90814008, 40921002, and 41090372), Opening Foundation of State Key Laboratory of Ore Deposit Geochemistry, Institute of Geochemistry, CAS (No. 2008011), and Fund for Mineral Exploration from Anhui Bureau of Land and Mineral Resources. We thank Prof. Chang Yinfo for his kind guidance.

References

Aguillón-Robles, A., Calmus, T., Benoit, M., Bellon, H., Maury, R.C., Cotten, J., Bourgois, J., and Michaud, F., 2001, Late Miocene adakites and Nb-enriched basalts from Vizcaino Peninsula, Mexico: Indicators of East Pacific rise subduction below southern Baja California? Geology, v. 29, p. 531–534.

Bi, X.W., Hu, R.Z., Peng, J.T., Wu, K.X., Su, W.C., and Zhang, X.Z., 2005, Geochemical characteristics of the Yao'an and Machangqing alkaline-rich intrusions: Acta Petrologica Sinica, v. 21, p. 113–124.

Bi, X.W., Hu, R.Z., Ye, Z.J., and Shao, S.X., 2000, Relations between A-type granites and copper mineralization as exemplified by the machangqing Cu deposit: Science in China Series D-Earth Sciences, v. 43, p. 93–102.

Bonin, B., Azzouni-Sekkal, A., Bussy, F., and Ferrag, S., 1998, Alkali-calci and alkaline post-erogenic (PO) granite magmatism: Petrologic constraints and geodynamic settings: Lithos, v. 45, p. 45–70.

Calmus, T., Pallares, C., Maury, R.C., Bellon, H., Perez-Segura, E., Aguillon-Robles, A., Carreno, A.L., Bourgois, J., Cotten, J., and Benoit, M., 2008, Petrologic diversity of Plio-Quaternary post-subduction volcanism in northwestern Mexico: An example from Isla San Esteban, Gulf of California: Bulletin de la Societe Geologique de France, v. 179, p. 465–481.

Cao, Y., Du, Y.S., Cai, C.L., Qin, X.L., Li, S.T., and Xiang, W.S., 2008, Mesozoic A-type granitoids and xenoliths in the Lujiang–Zongyang, Anhui Province: significance in post-collisional magmatic evolution: Geological Journal of China, v. 14, p. 565–576.

Castillo, P.R., 2008, Origin of the adakite–high Nb basalt association and its implications for postsubduction magmatism in Baja California, México: Geological Society of America Bulletin, v. 120, p. 451–462.

Chang, Y.F., Liu, X.P., and Wu, Y.C., 1991, The copper-iron belt of the middle and lower reaches of the Changjiang river: Beijing, Geological Publishing House, p. 1–379.

Chen, J.F., and Jahn, B.M., 1998, Crustal evolution of southeastern China: Nd and Sr isotopic evidence: Tectonophysics, v. 284, p. 101–133.

Chen, J.F., Yan, J., Zhi, X., Xu, X., and Xing, F.M., 2001, Nd and Sr isotopic compositions of igneous rocks from the lower Yangtze region in Eastern China: Constraints on sources: Physics and Chemistry of Earth (A), v. 26, p. 719–731.

Chen, J.F., Yu, G., Yang, G., and Yang, S.H., 2005, A geochronological framework of late mesozoic magmatism and metallogenesis in the lower Yangtze valley, Anhui Province: Geology of Anhui, v. 15, p. 161–169, (in Chinese with English abstract).

Chen, J.F., Zhou, T.X., Li, X.M., Foland, K.A., Huang, C.Y., and Lu, W., 1993, Sr and Nd isotopic constraints on source regions of the intermediate and acidic intrusions from southern Anhui province: Geochimica, v. 22, p. 26l–268.

Chung, S.L., 1999, Trace element and isotope characteristics of Cenozoic basalts around the Tanlu fault with implications for the eastern plate boundary between North and South China: The Journal of Geology, v. 107, p. 301–312.

Collins, W.J., Beams, S.D., White, A.J.R., and Chappell, B.W., 1982, Nature and origin of A-type granites with particular reference to southeastern Australia: Contributions to Mineralogy and Petrology, v. 80, p. 189–200.

Condie, K.C., 1982, Plate tectonics and crustal evolution: New York, Pergamon Press, 135 p.

Deng, J.F., Zhao, H.L., and Mo, X.X., 1996, Continental roots-plume tectonics of China: Key to the continental dynamics: Beijing, Science Press, 110 p. (in Chinese).

Deng, J.F., Ye, D.L., Zhao, H.L., and Tang, D.P., 1992, Volcanism, deep internal processes and basin formation in the lower reaches of the Yangtze River: Wuhan, Press of China University of Geosciences, p. 1–184.

Defant, M.J., and Drummond, M.S., 1993, Mount St. Helens: Potential example of the partial melting of the subducted lithosphere in a volcanic arc: Geology, v. 21, p. 547–550.

Defant, M.J., Jackson, T.E., Drummond, M.S., and De, B., 1992, The geochemistry of young volcanism throughout western

Panama and southeastern Costa Rica: An overview: Journal of the Geological Society, v. 149, p. 569–579.

Defant, M.J., Richerson, P.M., De, B., Jelle, Z., Stewart, R.H., Maury, R.C., Bellon, H., Drummond, M.S., Feigenson, M.D., and Jackson, T.E., 1991, Dacite genesis via both slab melting and differentiation: Petrogenesis of La Yeguada volcanic complex, Panama: Journal of Petrology, v. 32, p. 1101–1142.

Ding, X., Sun, W.D., Huang, F., Lundstrom, C., Li, J., Di, Wu, C., Sun, Y., Lin, C., Li, H., and Chen, L., 2007, Different mobility of Nb and Ta along a thermal gradient: Geochimica et Cosmochimica Acta, v. 71, p. A226–A226.

Eby, G.N., 1992, Chemical subdivision of the A-type granitoids; Petrogenetic and tectonic implications: Geology, v. 20, p. 641–644.

Engebretson, D.C., Cox, A., and Gordon, R.G., 1985, Relative motions between occanic and continental plates in the Pacific basin: The Geological Society of America Special Paper, v. 206,p . 1–59.

Fan, Y., Zhou, T.F., Yuan, F., Qian, C.C., Lu, S.M., and Cooke, D., 2008, LA-ICP-MS zircon U-Pb ages of the A-type granites in the Lu-Zong(Lujiang-Zongyang)area and their geological significance: Acta Petrologica Sinica, v. 24, p. 1715–1724. (in Chinese with English abstract).

Jahn, B.M., Wu, F.Y., and Lo, C.H., 1999, Crust-Mantle interaction induced by deep subduction of the continental crust: Geochemical and Sr-Nd isotopic evidence from post-collisional mafic-ultramafic intrusions of the northern Dabie complex,central China: Chemical Geology, v. 157, p. 119–146.

Harris, N.B.W., Pearce, J.A., and Tindle, A.G., 1986, Geochemical characteristics of collision zone magmatism: Geological Society, London, Special Publications, v. 19, p. 67–81.

Hofman, A., 1988, Chemical differentiation of the Earth: the relationship between mantle, continental crust, and oceanic crust: Earth and Planetary Science Letters, v. 90, p. 297–314.

Kepezhinskas, P., Defant, M.J., and Drummond, M.S., 1996, Progressive enrichment of island arc mantle by melt-peridotite interaction inferred from Kamchatka xenoliths: Geochimica et Cosmochimica Acta, v. 60, p. 1217–1229.

Li, H., Zhang, H., Ling, M.X., Wang, F.Y., Ding, X., Zhou, J.B., Yang, X.Y., Tu, X.L., and Sun, W.D., 2011, Geochemical and zircon U-Pb study of Huangmeijian A-type granite: Implications on the geological evolution of the lower Yangtze River belt: International Geology Reviews, v. 53, p. 499–525.

Li, Z.X., 1994, Collision between the North and South China blocks: A crustal-detachment model for suturing in the region east of the Tanlu fault: Geology, v. 22, p. 739–742.

Ling, M.X., Wang, F.Y., Ding, X., Hu, Y.H., Zhou, J.B., Zartman, R.E., Yang, X.Y., and Sun, W.D., 2009, Cretaceous ridge subduction along the lower Yangtze River belt, Eastern China: Economic Geology, v. 104, p. 303–321.

Liu, H., Qiu, J.S., Lo, C.-h, Xu, X.S., Ling, W.L., and Wang, D.Z., 2002, Petrogenesis of the Mesozoic potash-rich volcanic rocks in the Luzong basin, Anhui province: Geoehemical constraints: Geochimica, v. 31, p. 129–140. (in Chinese with English abstract).

Liu, S.A., Li, S.G., Teng, F.Z., He, Y.S., and Huang, F., 2010, Geochemical contrasts between early Cretaceous ore-bearingand ore-barren high-Mg adakites in central-eastern China: Implications for petrogenesis and Cu-Au mineralization: Geochimica et Cosmochimica Acta, v. 74, p. 7160–7178.

Loiselle, M.C., and Wones, D.R., 1979, Characteristics and origin of anorogenic granites: Geological Society of American Bulletin (Abstracts), v. 11, 468 p.

Mao, J.W., Wang, Y.T., Lehmann, B., Yu, J.J., Du, A.D., Mei, Y.X., Li, Y.F., Zang, W.S., Stein, H.J., and Zhou, T.F., 2006, Molybdenite Re-Os and albite Ar-40/Ar-39 dating of Cu-Au-Mo and magnetite porphyry systems in the Yangtze River valley and metallogenic implications: Ore Geology Reviews, v. 29, p. 307–324.

Maruyama, S., Isozaki, Y., and Kimura, G., 1997, Paleogeographic maps of the Japanese islands: Plate tectonic synthesis from 750 Ma to the present: Island Arc, v. 6, p. 121–142.

Middlemost, E.A.K, 1985, Magmas and magmatic rocks: London, Longman, 266 p.

Middlemost, E.A.K., 1994, Naming materials in the magmaligneous rock system: Earth Science Reviews, v. 37, p. 215–244.

Morrison, G., 1980, Characteristics and tectonic setting of the shoshonite rock association: Lithos, v. 13, p. 97–108.

Muller, D., and Groves, D.I., 1995, Potassic igneous rocks and associated gold-copper mineralization: New York, Springer-Verlag, Lecture Notes in Earth Sciences, v. 56, 210 p.

Palmer, H., 1968, East Pacific rise and westward drift of North America: Nature, v. 220, p. 341–345.

Pan, Y.M., and Dong, P., 1999, The lower Changjiang (Yangzi/Yangtze River) metallogenic belt, East central China: Intrusion- and wall rock-hosted Cu-Fe-Au, Mo, Zn, Pb, Ag deposits: Ore Geology Reviews, v. 15, p. 177–242.

Pearce, T.H., Gorman, B.E., and Birkett, T.C., 1977. The relationship between major element chemistry and tectonic environment of basic and intermediate volcanic rocks: Earth and Planetary Science Letters, v. 36, p. 121–132.

Pearce, J.A., Harris, N.B.W., and Tindle, A.G., 1984, Trace element discrimination diagrams for the tectonic interpretation of granitic rocks: Journal of Petrology, v. 25, p. 956–983.

Peccerillo, A., and Taylor, S., 1976, Geochemistry of Eocene calk-alkaline volcanic rocks from the Kastamonu area, northern Turkey: Contributions to Mineralogy and Petrology, v. 58, p. 63–81.

Petford, N., and Atherton, M., 1996, Na-rich partial melts from newly underplated basaltic crust: The Cordillera Blanca Batholith, Peru: Journal of Petrology, v. 37, p. 1491–1521.

Reagan, M.K., and Gill, J.B., 1989, Coexisting calcalkaline and high-niobium basalts from Turrialba volcano, Costa Rica: Implications for residual titanates in arc magma sources: Journal of Geophysical Research, v. 94, p. 4619–4633.

Ren, Q.J., Liu, X.S., and Xu, Z.W., 1991, Luzong volcanic basin of Mesozoic era and the mineralization, Anhui, East China: Beijing, Geological Publishing House, p. 1–206. (in Chinese with English Abstract).

Rudnick, R., and Fountain, D., 1995, Nature and composition of the continental crust: A lower crustal perspective: Reviews of Geophysics, v. 33, p. 267–309.

Rudnick, R.L., and Gao, S., 2003, Composition of the continental crust, in Holland, H.D., and Turekian, K.K., eds., Treatise on geochemistry, Volume 3: Oxford, UK, Elsevier, p. 1–64.

Sajona, F.G., Maury, R.C., Bellon, H., Cotten, J., and Defant, M.J., 1996, High field strength element enrichment of Pliocene–Pleistocene island arc basalts, Zamboanga Peninsula, Western Mindanao (Philippines): Journal of Petrology, v. 37, p. 693–726.

Sajona, F.G., Bellon, H., and Maury, R.C., 1994, Magmatic response to abrupt changes in geodynamic settings: Pliocene-Quaternary calcalka-line lavas and Nb enriched basalts of Leyte and Mindanao (Philippines): Tectonophysics, v. 237, p. 47–72.

Sajona, F.G., Maury, R.C., Bellon, H., Cotten, J., Defant, M.J., and Pubellier, M., 1993, Initiation of subduction and the generation of slab melts in western and eastern Mindanao, Philippines: Geology, v. 21, p. 1007–1010.

Sun, S.S., and McDonough, W.F., 1989, Chemical and isotopic systematics of oceanic basalts: Implications for mantle composition and processes: Geological Society London Special Publications, v. 42, 313 p.

Sun, W.D., Ding, X., Hu, Y.H., and Li, X.H., 2007, The golden transformation of the cretaceous plate subduction in the West Pacific: Earth Planet Science Letters, dio: 10.1016/j.epsl.2007.08.021.

Tang, Y.C., Wu, Y.C., Chu, G.Z., Xing, F.M., Wang, Y.M., Cao, F.Y., and Chang, Y.F., 1998, Geology of copper-gold polymetallic deposits along the Yangtze River, Anhui Province: Beijing, Geological Publishing House, p. 1–351.

Thorkelson, D.J., 1996, Subduction of diverging plates and the principles of slab window formation, Tectonophysics, v. 255, p. 47–63.

Thorkelson, D.J., and Breitsprecher, K., 2005, Partial melting of slab window margins: Genesis of adakitic and non-adakitic magmas; Lithos, v. 79, p. 25–41.

Viruete, J.E., Contreras, F., Stein, G., Urien, P., Joubert, M., Perez-Estaun, A., Friedman, R., and Ullrich, T., 2007, Magmatic relationships and ages between adakites, magnesian andesites and Nb-enriched basalt-andesites from Hispaniola: Record of a major change in the Caribbean island arc magma sources: Lithos, v. 99, p. 151–177.

Wang, D.Z., Zhou, J.C., and Qiu, J.S., 1991, Recently research of shoshonite series: Journal of Nanjing University (Natural Sciences), v. 1, p. 1–10. (in Chinese with English abstract).

Wang, D.Z., Zhao, G.T., and Qiu, J.S., 1995, The tectonic constraint on the late Mesozoic A-type granitoids in eastern China: Geological Journal of China Universities, v. 1, p. 13–21. (in Chinese with English abstract).

Wang, D.Z., Ren, Q.J., Qiu, J.S., Chen, K.R., Xu, Z.W., and Zeng, J.H., 1996, Characteristics of volcanic rocks in the shoshonite province, Eastern China and their metallogenesis: Acta Geologica Sinica, v. 70, p. 23–34. (in Chinese with English abstract).

Wang, Q., Zhao, Z.H., Xiong, X.L., and Xu, J.F., 2001, Melting of theunderplated basaltic lower crust: Evidence from Shaxi adakitic sodic quartz dirorite-porphyrites, Anhui province, China: Geochimica, v. 30, p. 353–362, (in Chinese with English abstract).

Wang, Q., Xu, J.F., Zhao, Z.H., Xiong, X.L., and Bao, Z.W., 2003, Petrogenesis of the Mesozoic intrusive rocks in the Tongling area, Anhui Province, China and their constraint on geodynamic process: Science in China Series D-Earth Sciences, v. 46, p. 801–815.

Wang, Q., Wyman, D.A., Xu, J.F., Zhao, Z.H., Jian, P., Xiong, X.L., Bao, Z.W., Li, C.F., and Bai, Z.H., 2006, Petrogenesis of Cretaceous adakitic and shoshonitic igneous rocks in the Luzong area, Anhui Province (Eastern China): Implications for geodynamics and Cu-Au mineralization: Lithos, v. 89, p. 424–446.

Wang, Y., Deng, J.F., and Ji, G.Y., 2004, A perspective on the geotectonic setting of early Cretaceous adakite-like rocks in the lower reaches of Yangtze River and its significance for copper-gold mineralization: Acta Petrologica Sinica, v. 20, p. 297–314. (in Chinese with English abstract).

Whalen, J.B., Currie, K.L., and Chappell, B.W., 1987, A-type granites: Geochemical characteristics, discrimination and petrogenesis: Contributions to Mineralogy and Petrology, v. 95, p. 407–419.

Whittaker, J.M., Müller, R.D., Sdrolias, M., and Heine, C., 2007, Sunda-Java trench kinematics, slab window formation and overriding plate deformation since the Cretaceous: Earth and Planetary Science Letters, v. 255, p. 445–457.

Wong, J., Sun, M., Xing, G., Li, X.H., Zhao, G., Wong, K., Yuan, C., Xia, X., Li, L., and Wu, F., 2009, Geochemical and zircon U-Pb and Hf isotopic study of the Baijuhuajian metaluminous A-type granite: Extension at 125–100 Ma and its tectonic significance for South China: Lithos, v. 112, p. 289–305.

Wu, C.L., Chen, S.N., Shi, R.D., and Hao, M.Y., 2003, Origin and features of the Mesozoic intermediate-acid intrusive rocks in the Tongling area, Anhui, China: Acta Geoscientia Sinica, v. 24, p. 41–48. (in Chinese with English abstract).

Wu, L.R., and Qi, J.Y., 1985, The Mesozoic volcanic rocks along the lower reaches of Yangtze River region, *in* Institute of Geology, A.S., ed., Petrological research: Beijing, Science Press, p. 1–10, (in Chinese with English abstract).

Xiao, Y.L., Sun, W.D., Hoefs, J., Simon, K., Zhang, Z., Li, S.G., and Hofmann, A.W., 2006, Making continental crust through slab melting: Constraints from niobium–tantalum fractionation in UHP metamorphic rutile: Geochimica et Cosmochimica Acta, v. 70, p. 4770–4782.

Xie, Z., Li, Q.Z., Chen, J.F., and Shan, G.T., 2007, The geochemical characteristics of the Early-Cretaceous volcanics in luzong region and their source significances: Geological Journal of China Universities, v. 13, p. 235–249. (in Chinese with English abstract).

Xing, F.M., and Xu, X., 1995, The essential features of mamatic rocks along the Yangtze River in Anhui province: Acta Petrologica Sinica, v. 11, p. 409–420. (in Chinese with English abstract).

Xing, F.M., and Xu, X., 1996, High-potassium calc-alkaline intrusive rocks in Tongling area, Anhui province: Geochimica, v. 25, p. 29–38. (in Chinese with English abstract).

Xing, F.M., and Xu, X., 1998, The characteristics and origin of the shoshonites around the Yangtze river reaches of Anhui – An example from continental shoshonitic rock series: Geology of Anhui, v. 8, p. 8–20 (in Chinese with English abstract).

Xing, F.M., and Xu, X., 1999, Yangtze magmatic belt and metallogenesis: Hefei, Anhui People's Publishing House, p. 1–170. (in Chinese).

Xu, J.W., and Zhu, G., 1994, Tectonic models of the Tan-Lu fault zone, Eastern China: International Geology Review, v. 36, p. 771–784.

Xue, H.M., and Tao, K.Y., 1989, New view on the mesozoic volcanic sequences in Ning-Wu: Jiangsu Geology, v. 13, p. 9–14. (in Chinese with English abstract).

Yang, R.Y., Ren, Q.J., Xu, Z.W., Sun, Y.D., Guo, G.Z., and Qiu, J.S., 1993, The magma source of Bajiatan volcanic-intrusive complex in the Lujiang-Zhongyang area, Anhui province: Geochemica, v. 2, p. 197–206. (in Chinese with English Abstract).

Yang, R.Y., Ren, Q.J., Xu, Z.W., and Xu, L., 1996, The Bajiatan volcanic dome in the mesozoic volcanic terraln of the Lujiang-Zongyang area, Anhui province: Geological Review, v. 42, p. 136–143. (in Chinese with English abstract).

Yang, X.Y., 1996, The Cu-Au metallogenic prospecting areas from middle-lower reaches of Changjiang river: A study on metallogenic geochemistry of some typical copper and gold ore deposits [Ph.D. dissertation]: Hefei, University of Science and Technology of China, p. 1–214. (in Chinese with English abstract).

Yang, X.Y., and Lee, I.S., 2005, Geochemistry and metallogenesis in lower part of Yangtze metallogenic valley: A case study in Shaxi-Changpushan porphyry Cu-Au deposit and a review on the adjacent Cu-Au deposits: Neues Jahrbuch für Mineralogie (Abh.), v. 181, p. 223–243.

Yang, X.Y., Wang, K.R., Yang, X.M., and Sun, L.G., 2002, Characteristics of mineralization and gold occurrence in Shaxi porphyry copper-gold deposit, central Anhui, China: Neues Jahrbuch für Mineralogie (Abh), v. 177, p. 293–320.

Yang, X.Y., Yang, X.M., Jiang, L.L., Wang, K.R., and Sun, L.G., 2006, Trace element geochemistry of some Mesozoic Yanshanian copper-gold deposits on Anhui middle-lower Yangtze metallogenic valley, central-east China: Journal of The Geological Society of India, v. 67, p. 475–494.

Yang, X.Y., Zheng, Y.F., Du, J.G., Xiao, Y.L., and Sun, W.D., 2007, $^{40}Ar/^{39}Ar$ dating of Shaxi porphyry Cu-Au deposit, South Tancheng-Lujiang fault belt, Anhui Province: Acta Geologica Sinica, v. 76, p. 801–812.

Yang, X.Y., Yang, X.M., Zhang, Z.W., Chi, Y.Y., Yu, L.F., and Zhang, Q.M., 2011, A porphyritic copper (gold) ore-forming model for the Shaxi-Changpushan district, lower Yangtze metallogenic belt, China: Geological and geochemical constraints: International Geology Reviews, v. 53, p. 741–757.

Yu, X.Y., and Bai, Z.H., 1981, Trachyandesite series in Luzong, Anhui: Geochemica, v. 10, p. 57–65. (in Chinese with English abstract).

Yuan, F., Zhou, T.F., Fan, Y., Lu, S.M., Qian, C.C., Zhang, L.J., Duan, C., and Tang, M.H., 2008, Source, evolution and tectonic setting of Mesozoic volcanic rocks in Luzong basin, Anhui Province: Acta Petrologica Sinica, v. 24, p. 1691–1702.

Zhai, Y.S., Xiong, Y.L., Yao, S.Z., and Lin, X.D., 1996, Metallogeny of copper and iron deposits in the Eastern Yangtze Craton, East-central China: Ore Geology Reviews, v. 11, p. 229–248.

Zhai, Y.S., Yao, S.Z., Lin, X.D., Zhou, X.R., Wan, T.F., Jin, F.Q., and Zhou, Z.G., 1992, Metallogeny of Iron and copper (gold) deposits in the middle-lower reaches of Yangtze River: Beijing, Geological Publishing House, p. 1–235. (in Chinese).

Zhang, B.T., Zhang, F.S., Ni, Q.S., Chen, P.R., Zhai, J.P., and Shen, W.Z., 1988, Geology and geochemical characteristics of the Anqing-Lujiang Quartz syenite rock-belt and its genesis: Acta Petrologica Sinica, v. 4, p. 1–12. (in Chinese with English abstract).

Zhang, H.X., Zhang, B.Y., and Niu, H.C., 2005, Nb-enriched basalt: The product of the partial melting of the slab-derived melt metasomatized mantle peridotite: Advances in Earth Science, v. 20, p. 1234–1242. (in Chinese with English abstract).

Zhang, H.F., Gao, S., Zhang, B.R., Luo, T.C., and Ling, W.L., 1998, Pb isotopes of granitoids suggest Devonian accretion of Yangtze (South China) craton to North China craton: Reply: Geology, v. 26, p. 860–861.

Zhang, Q., Jian, P., Liu, D.Y., Wang, Y.L., Qian, Q., Wang, Y., and Xue, H.M., 2003, SHRIMP dating of the zircons in volcanic rocks from Ning-Wuhu area and its implications: Science in China (Series D), v. 33, p. 309–314. (in Chinese with English abstract).

Zhao, Z.H., Tu, G.C., and Xu, J.F., 2003, Super deposits in China(II)[M]: Beijing, Science Press, 617 p. (in Chinese).

Zhao, Z.H., Wang, Q., and Xiong, X.L., 2004, Complex mantle-crust interaction in subduction zone: Bulletin of Mineralogy, Petrology and Geochemistry, v. 23, p. 277–284. (in Chinese with English abstract).

Zheng, Y.F., Wei, C.S., and Wang, Z.R., 1997, An isotope study on the cooling history of the Dalongshan granitic massif and its bearing on mineralizing process: Scientia Geologica Sinica, v. 32, p. 465–477. (in Chinese with English abstract).

Zhou, T.F., Song, M.Y., Fan, Y., Yuan, F., Liu, J., Wu, M.A., Qian, C.-C., and Lu, S.-M., 2007, Chronology of the Bajiatan intrusion in the Luzong basin, Anhui, and its significance: Acta Petrologica Sinica, v. 10, p. 2379–2386. (in Chinese with English abstract).

Zhou, T.F., Yu, F., and Yuan, F., 2008, Advances on petrogensis and metallogeny study of the mineralization belt of the middle and lower reaches of the Yangtze River area: Acta Petrologica Sinica, v. 24, p. 1665–1678. (in Chinese with English abstract).

Zhu, G., Liu, G.S., Niu, M.N., Song, C.Z., and Wang, D.X., 2003, Transcurrent movement and genesis of the Tan-Lu fault zone: Regional Geology of China, v. 22, p. 200–212. (in Chinese with English abstract).

Zindler, A., and Hart, S.R., 1986, Chemical Geodynamics: Annual Review of Earth and Planetary Sciences, v. 14, p. 753–775.